FACULTAD DE CIENCIAS DEL MAR

UNIVERSIDAD DE LAS PALMAS DE GRAN CANARIA

PALEOGEOMORFOLOGICAL RECONSTRUCTION AND MODELING OF HOLOCENE VOLCANISM IN THE CANARY ISLANDS USING GIS TOOLS

Airam Echedey Pérez Reyes

Academic year 2018/2019

Tutor: Alejandro Rodríguez González

Final Degree Project to obtain the title of Graduated in Marine Sciences

Final degree project title:

Paleogeomorfological reconstruction and modeling of Holocene volcanism in the Canary Islands using GIS tools.

Student data:

- ✓ **Name:** Airam Echedey
- ✓ **Surname:** Pérez Reyes
- ✓ **Titling:** Degree in Marine Sciences
- ✓ **Grade:** 4th

Tutor data:

- ✓ **Name:** Alejandro
- ✓ **Surname:** Rodríguez González
- ✓ **Department:** Physics (Geology)
- ✓ **Research group:** GEOVOL (i-UNAT)

Date and signature:

Student: Airam Echedey Pérez Reyes

Tutor: Alejandro Rodriguez González

June 2019

ACKNOWLEDGEMENTS

This Final Degree Work (FDW) has been carried out at the University of Las Palmas of Gran Canaria (Faculty of Marine Sciences), through personal dedication with a view to a successful future work. However, I must say that this merit isn't mine, but to those people who have allowed the development of my academic career from the begins. From my point of view, an FDW is the culmination of several years of studies. Fortunately or unfortunately, with its good and bad days, and if they hadn't been, I couldn't have overcome even the first obstacle.

Firstly, I would like to give my most sincere thanks to my FDW tutor, Dr. Alejandro Rodríguez González. Because he has endured my constant queries since the work began and has given me the necessary answers for the continuity of the work. I thank him for his dedication to me as a mentor and guide during these intense months. Without him I would have been lost and I wouldn't have even found his complete thesis, which has helped me a lot.

Besides, other teachers such as Dr. Mª del Carmen Cabrera Santana and Dr. Francisco José Pérez Torrado also deserve a special mention as thanks for giving me basic knowledge, not only about geology, but also a good sanity and humility. They revived my passion for the natural sciences.

On the other hand, I cannot conclude this stage of my life without saying a few words about the companions of Marine Sciences. On the presenting day, four years ago, a veteran student had told us that the faculty is like a big family. At that time, I didn't understand it, but months passed and the answer came to me. The companionship grade that can be reached is such that one can reach friendships and contacts for a lifetime because the hard obstacles in the way (jobs, partial exams, reports, homework, etc.) we overcome them with help from each other.

Finally, for helping me find the right path, achieve my purpose in life and always be offering their support, not only in my successes but also in my failures, I thank with all my heart to my family, my parents, my sister, my grandparents and my life partner, your patience and trust in me.

The pride in this work must belong both they and me.

INDEX

FIGURES INDEX

Page

6. MODELING LAVA FLOWS

7. Q-LAVHA AND ITS INTEGRATION TO SIMULATION MODELS

8. PICO DE BANDAMA LAVA FLOW SIMULATION ANALYSIS

9. CONCLUSIONS

TABLES INDEX

1. INTRODUCTION

Volcanic activity has influenced the development of human species since immemorial time, either positively and negatively. The Canary Islands are no exception, as they have a purely volcanic nature. Lava flows, pyroclastic flows, debris avalanches, lahars and landslides are typical gravitational processes that can destroy a natural environment. As human species may be present in this environment, there is a high possibility that he life, health and belongings of people suffer some damage during these processes. This is a real hazard in nearby settlements in areas with volcanic activity.

The high fertility of volcanic terrains is the main reason why many cities have grown in these risky areas. Two good examples are: Naples in Italy and Kagoshima in southern Japan that are under the Mount Vesuvius and Mount Sakurajima, respectively (Fig. 1.1 A-D). The high porosity particles, which characterize the soil of the volcanic terrains, are enriched by magnesium, potassium and nutrients. It is making them more useful and incrementing the risk of a possible catastrophe.

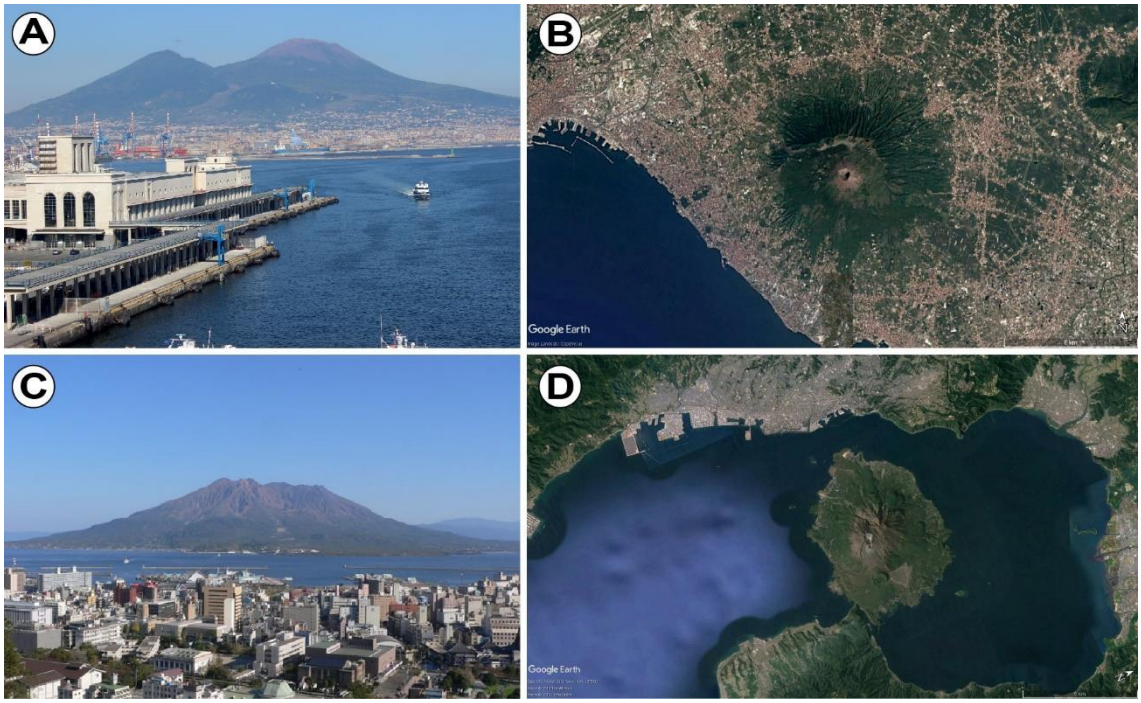

Figure 1.1 Examples of urban development in the vicinity of high-hazard volcanoes. A) Naples city view at the foot of Mount Vesuvius. B) Satellite image of Naples and other county terms surrounding the volcano. C) Kagoshima city view next to Sakurajima volcano. D) Satellite view of Kagoshima Bay with the volcano in the middle (Source: Wikimedia commons and Google Earth).

Nowadays, it is very important to understand the geological processes that are behind each volcano in order to protect people. Thus, it is proposed to do research on volcanism based on Geographic Information Systems (GIS). With the purpose of

obtaining the necessary information and gaining knowledge about the future behavior of a particular volcano. This research may be a powerful tool in volcanology that allow to combine different results such as topographies, chronology and rock composition, morphologies and description of volcanic structures. They produce more accurate interpretations. These results are inserted in a database dedicated to represent the volcano evolution in space and time. Consequently, the information is available in the form of thematic maps, which address issues such as the eruption virulence, their action range and the possible regional distribution of ejected materials (ash, lava flows and pyroclastic flows). The result is a very useful data for the authorities because it allows to assess and manage volcanic risks and to develop emergency plans.

This work is mainly focused on lava flows, chosen from all volcanic hazardous areas since the geological record shows that they are the most common in Gran Canaria. The greatest danger associated with lava flows are associated with fires and burial damage. In this regard, the people have attempted in many occasions to control the lava flow advance using different methods (barriers, diversion channels, deviation induced destruction of lava tunnels, cooling flows through water jets, etc.) but in most cases they have ended in failure.

In recent years, there has been a great development of eruptive processes modeling and simulation, which allows increasing the knowledge about future eruptions: possible affected areas by its eruptive products, when they will take place and how. The most correct way to answer these points is through producing thematic maps representing the distribution of volcanic hazards (Fig. 1.2) displaying all the information gained from detailed research ~~o~~f past volcanic eruptions together with the predictions new models of lava flow.

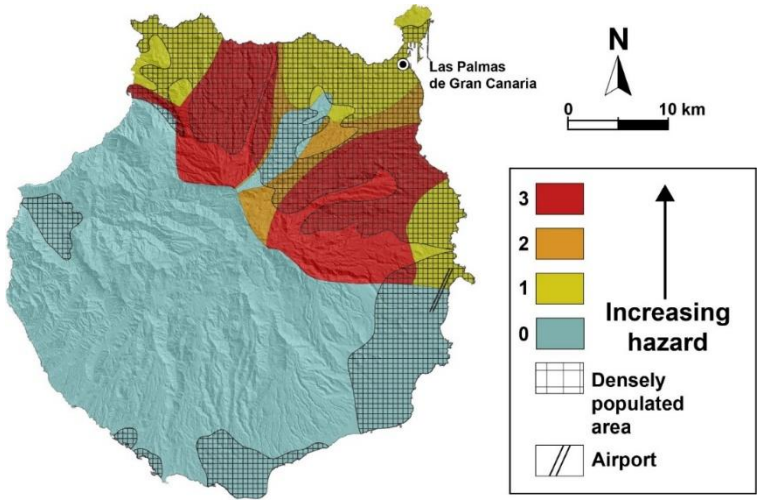

Figure 1.2 Volcanic hazard map of Gran Canaria. (Modified from Rodríguez-González, 2009).

In the following work, the numerical simulation of Pico de Bandama lava flows, from a set of parameters characterizing this eruption, will have special emphasis. However, the challenge of numerical models is the software optimization to reduce the execution's times of these simulations, which gives the best approximation to reality. Due to the large number of models developed during the recent years, both deterministic (mainly focused on the physical-chemical characteristics of lava flows) and probabilistic models (assuming that topography plays the most important role in the control of lava flows), will be used to compare the results applying Q-LavHA (*Quantum-Lava Hazard Assessment*). The Q-LavHA works under a GIS software, formerly called Quantum GIS (QGIS).

Finally, it will be possible to assess the effects of any eruption in any place and in a determined time. The GIS methodology allows it while it applied to the most recent example of Holocene volcanism in Gran Canaria.

2. THE GEOGRAPHIC INFORMATION SYSTEMS

The imported data into a GIS include geometric and topological descriptions of defined geographic entities. Therefore, "the geographic datum" is composed of fundamental information loaded in a GIS, because it describes the real world objects in terms of coordinates (spatial information). However, determined attributes (non-geographic or thematic information) can also be associated with spatial data. These systems are able to give the basic knowledge about positions on a coordinate system: the associated location attributes and the spatial relationships of objects with the surrounding geographic features. This allows a GIS to be a very effective tool for the geographic information management (Rodríguez-González, 2009).

Geographic data registration in a GIS database implies specific methodologies for inserting data in the system. A software administration technique problem because of the necessity to learn how to apply the methodologies mentioned above. However, how the quality of the information collected and the specifications of the equipment used influence cannot be forgotten. The importance of these factors is reduced to "geographic datum" volume and its complexity depending on the resolution. Thus, requiring to take the maximum optimization of the data, which becomes into a more efficient computational process.

"The geographic datum" is the most important in a GIS, but alphanumeric data are also useful, which remain linked to them through identifiers or other software mechanisms. Furthermore, the information is composed in vector mode (points, lines, polygons referred to georeferenced thematic attributes) and raster mode (pixel meshes or cells of a single theme) that represent geographic entities on maps directly.

From a more conceptual point of view, the interpretation of the results can lead to some major headaches due to its ambiguity. A common example could be to specify river limits in an estuary: it is not known exactly where it ends and the coast begins are. It is said that it is multiform, chameleonic, because depending on the user's needs, it can acquire very different appearances. The key word to this technology is Geography; which usually means that data (or at least a certain proportion of the data) are spatial. Meaning, that data are related to its locators in the field in a certain way (Rodríguez-González, 2009).

The definition of a GIS encompasses the concept of Information Systems (IS). Not necessarily computer procedures, whose function is to answer indeterminate questions. Hence, the term CBS (Computer Based System) is used more frequently

because computers have a great weight in GIS. At the same time, a geo-referenced database is defined with geographic information (Rodríguez-González, 2009), characterized by its functionality (Burrough, 1986, Clarke, 1986, Department of the Environment, 1987, and NCGIA, 1990) and used as a support when making decisions (Cowen, 1988). This implies a set of procedures for analyzing and manipulating data by a system of interaction with the user or interface.

The most basic level of a GIS (Fig. 2.1) consists of a computer cartography: the composition of digital maps, which in a simple way capture all the information loaded in the database. In addition, GIS is commonly called/named "visual database". However, its true potential use spatial and statistical methods to analyze attributes and geographic information. The final analysis result can be derived information, interpolated information or priority information (Antenucci, 1991). Its ability to generate new information derived from original data, through its manipulation and reworking (Dunker, 1987 and Cowen 1988), is a distinctive feature with respect to other computer mapping programs.

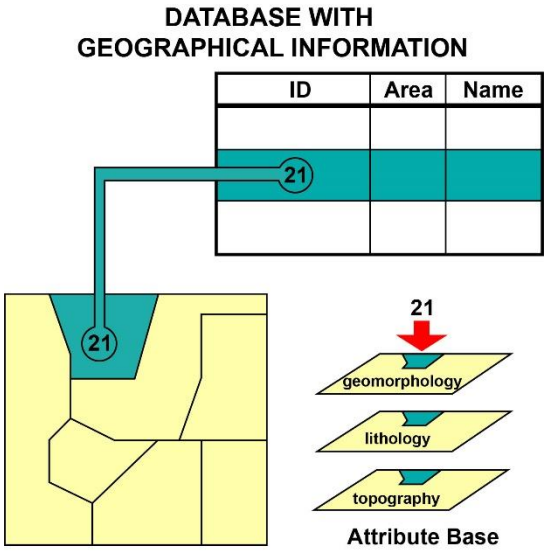

Figure 2.1. GIS levels by layers

GIS is a technical discipline with an important theoretical section and a well-differentiated methodology. The development of any GIS project requires pre-established conditions; a general methodology. A project is understood as the different realizations or practical of geographic information available. Firstly, it can be addressed starting with project conception, where user's needs and GIS requirements are defined. Subsequently/Secondly, a work proposal and an implementation plan (design) are drawn up. After that, the development is carried out, which covers aspects related to GIS components acquisition, as well as user applications configuration. Once completed,

operation proceeds establish the relevant processes with the aim of automating and optimizing tasks. At the same time, the project's progress is reviewed, including the possibilities of expansion or evolution to a more complete version for the future.

In conclusion, a GIS provides a territory dynamic view, allowing to handle a lot of information in a controlled way, and to integrate multiple approaches, whether different or complementary. Thus, the particular investigation results and conclusions, can be transmitted to public/people in a didactic and easy interpretation way.

3. THE VOLCANISM OF GRAN CANARIA

Gran Canaria island is a part of the Canary Volcanic Province (Fig. 3.1). This set of islands, islets and seamounts is located in the North Atlantic Ocean, in the Macaronesia region and off the coast of Morocco. The Canary Islands are located between 29° 25′ and 27° 37′ N and 18° 10′ and 13° 20′ W. This location is characterized by a geodynamic scenario marked by intraplate volcanic activity. It is characterized like that because volcanoes aren't produced in edges of tectonic plates. In Pacific Ocean, the Hawaii Islands face the same situation.

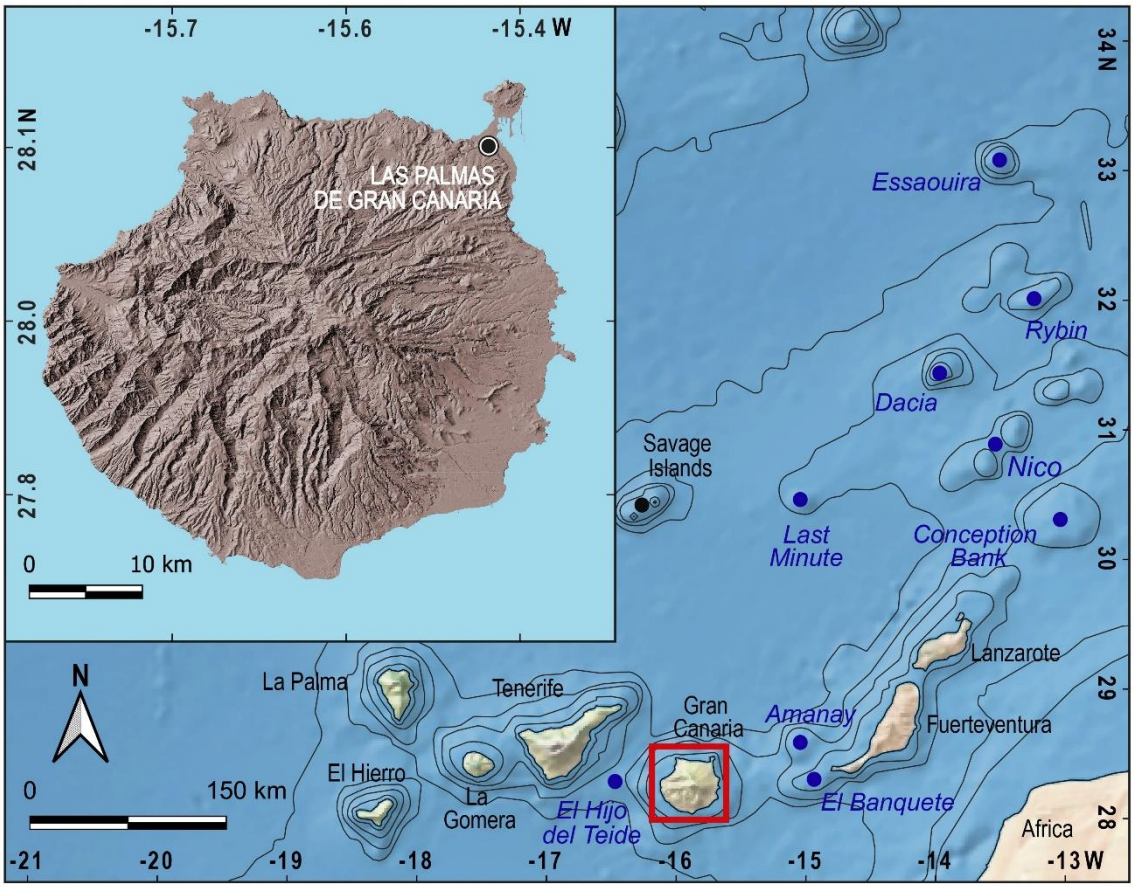

Figure 3.1. The Canary Islands and Gran Canaria location map.

The volcanic origin of the Canary Islands has been explained by various theories, from a propagating fracture from Atlas Mountains in continental Africa, until raised blocks existence. This blocks dragged ocean floor parts ocean with them to the surface, producing decompression and magma generation under the same. Instead, hypothesis proposed by Morgan (1973) has been accepted more widely, beginning with Wilson's (1963) intraplate volcanic islands investigations. His idea consists in a mantle plume (hotspot) as the mechanism of origin, it transports heat and material through an ascending flow to the asthenosphere. At the same time, African plate rotates on its rotation pole

($43°N\ 24°W$) and moves from SO to NE over the hotspot (0.12 cm/year). This movement leaving an islands line in its path (ENE-OSO). So, the oldest island building in the Canarian Archipelago is Fuerteventura-Lanzarote with 20.2 Ma (Millions of years old) approximately and the youngest, El Hierro with 1.1 Ma (Carracedo, 2011).

Each island has a balance between growth and erosion from its birth moment to present. The first process was developed by volcanic activity and the second, it was through external geological agents. It highlights the coastal hydrodynamics and the rainfall because they cause most of erosion.

3.1. The volcanic stratigraphy of Gran Canaria

Gran Canaria island approximates the typical standard development proposed by Walker (1990) for the intraplate volcanic islands. This model includes various stages: a first stage of underwater growth, a second juvenile and a rejuvenation last one or post-erosion. But, chronostratigraphy has described completely the subaerial growth cycles in detail.

- **Underwater Growth time.** Since there are not outcrops for visualize of the island's underwater roots, as in La Palma, Fuerteventura and more doubtfully in La Gomera (Carracedo, 2011), the first three formations submarine phases have got theoretical basics.
  - **Submarine stage I.** The submarine build formation begins with igneous intrusions: dike and sill types, in the rocky/sedimentary substrate of the oceanic crust. Occasionally, material emerges by means of low explosive eruptions spilling large diameter pillow-lavas.
  - **Submarine stage II:** The basal complex grows in terms of height and volume. Pillow-lavas stacking lose size while they ascend and they continue to intrude magmas through internal cracks in the building, filling them up to 50% of total volume.
  - **Emerging stage (the most studied):** There are data from ODP program (Leg 157) oceanographic campaigns demonstrating that this stage supposes more than 90% of the total island volume. It existed a uninterrupted activity while Gran Canaria came to the surface. Only a change occurred in the type of eruption: from shallow water eruptions, less than 500 meters deep, to a hydromagmatic volcanic activity, very explosive (Fig. 3.2 [1]). This was due to the fact that hydrostatic pressure wasn't enough to retain violent material expulsion, result of water-magma interaction. On the other hand, consecutive subaerial materials

geochemistry and their disposition indicated a common magmatic source for this material and the previous one (Rodríguez-González, 2009).

- **Juvenile state** (14.5 Ma - 8.8 Ma): It represents Gran Canaria development bulk with three main phases including shield volcano construction and exceptional processes, like Caldera de Tejeda formation and collapse and subsequent volcanic activity.
  - **Shield formation stage** (Fig. 3.2 [2-4]). It is a practically continuous lava stacking characteristic of Hawaiian magmatic activity with a summit area towards the west-center of island. A shield volcano with 2000 meters estimated height and approximate dimensions of actual Gran Canaria was formed. During this quick episode, gravitational landslides could occur at SO and NO regions (Rodríguez-González, 2009).
  - **Collapsing caldera** (Fig. 3.2 [5]). During the last basalt eruption of shield building, it was possible that a magma chamber could have been generated approximately 4-5 kilometers deep with a more acidic composition due to differentiation (alkaline decline). Renovations with deeper material could origin highly explosive eruptions of trachyte-rhyolitic material. Pouring of ignimbritic lava flows and the quick magmatic chamber emptying allowed chamber ceiling collapse. A great block sank dragging with him the island summit. It created an elliptical depression of 35x20 km and 1000 meters deep. At the same time, magma emerged by new cracks in caldera edges with new ignimbritic eruptions that covered part of the shield building.
  - **Post-caldera volcanism** (Fig. 3.2 [6-7]). There were eruptions along caldera edges that filled part of it and spilled large quantities of rhyolitic lavas at first ($14 - 13.3$ Ma) and trachytes-phonolites later ($13.3 - 8.8$ Ma). It is possible highlight that igneous intrusions in rhyolitic lavas take place in intra-caldera domain. By injection order, there are alkaline Sienites, a cone-sheet formation and phonolitic-nepheline domes, following previous philonian system external geometry.

Between juvenile state and the next one, Gran Canaria enters in an **erosion and volcanic inactivity stage** (Fig. 3.2 [8]) for more than 3 Ma. During this phase a ravine radial network and the "Las Palmas Detrital Formation" (LPDF) sedimentary deposits was built.

- **Rejuvenated stage** (5.5 Ma – Present day). Gran Canaria volcanic reactivation was characterized by the formation of a large stratovolcano at island center and development of small eruptive centers later.

- **Roque Nublo stratovolcano** (Fig. 3.2 [9-10]). This phase began with a dispersed volcanic activity; strombolian eruptions that later moved towards central areas of the island for 1.5 Ma. There the Roque Nublo stratovolcano was built, whose first eruptions spilled basaltic-basaitic lavas that were channeled through paleo-ravines, reaching the sea at north coast. Over time Roque Nublo volcano behavior becomes more explosive (Vulcanian-phreatomagmatic eruptions) with powerful ignimbritic emission, due to the composition of magma differentiated to trachytic-phonolitic. At the end of its development, they intruded numerous phonolitic domes and were produced gravitational landslides that dismantle building to a great extent.
- **Post-Roque Nublo volcanism** (Fig. 3.2 [11-12]). Volcanic activity in this phase was characterized by strombolian eruptions associated with a rift-type structure with NO-SE orientation. They originate a pyroclastic cones series between which they were spilled successive lava flows of basaitic-nefelinitic to traquibasaltic composition (Rodríguez- González, 2009). From 1.9 Ma on-wards rift volcanism pattern gives way to a very basic volcanic activity dispersed both spatially and temporally and characterized by strombolian cones and monogenetic phreatomagmatic calderas appearance.

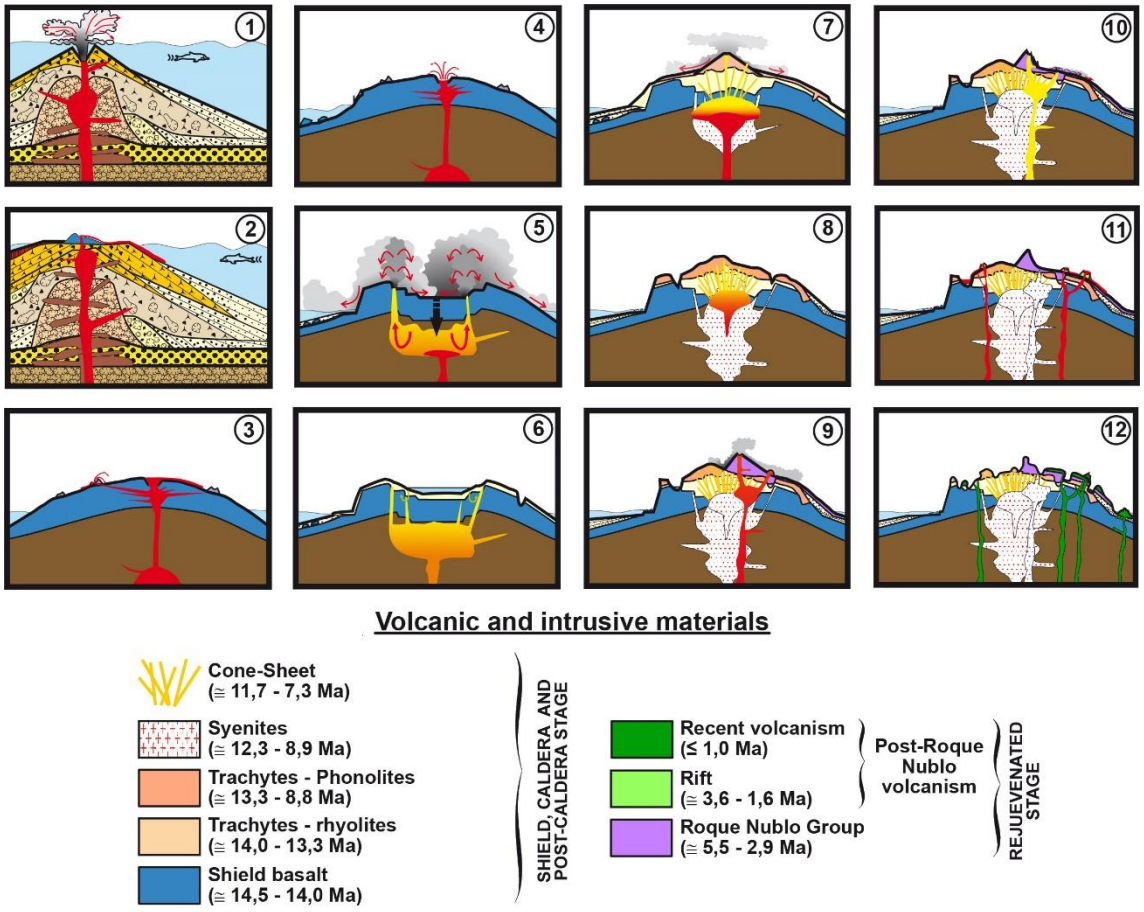

Figure 3.2. Volcanic evolution of Gran Canaria (modified from Rodríguez González, 2009).

Finally, the island is exposed to external geological agents, so there is **a last stage of erosion** to present days. There isn't a subsidence as stated in original model for Hawaii Islands. This is not applicable to Canary Islands because volcanic buildings settle on a plate very thick, supporting a great weight and preventing subsidence. However, erosion does work by lowering relief to turn it into smooth plains.

3.2. The Holocene volcanism of Gran Canaria: Pico de Bandama eruption case study

Gran Canaria island is in the last stage of all known volcanic activity, which covers present time (Holocene). A phase included in volcanic rejuvenated stage, the post-Roque Nublo cycle and, in turn, recent volcanism (Guillou et al., 2004). During this time, 24 similar characteristics eruptions (strombolian and phreato-strombolian cones) were generated. They centred on the north and northeast island sectors (Fig. 3.3), whose volcanic buildings were arranged following an apparent alignment trend NO-SE. The reason for this arrangement it explains for typical rift model in oceanic volcanic islands. However, it also has importance the giant landslides influence on tectonics, La Isleta building location by stabilizing the northern flanks and Tenerife island weight on Gran Canaria basal complex. This fact could be causing the tilting of the island (tilting) towards west (Rodríguez-González, 2009).

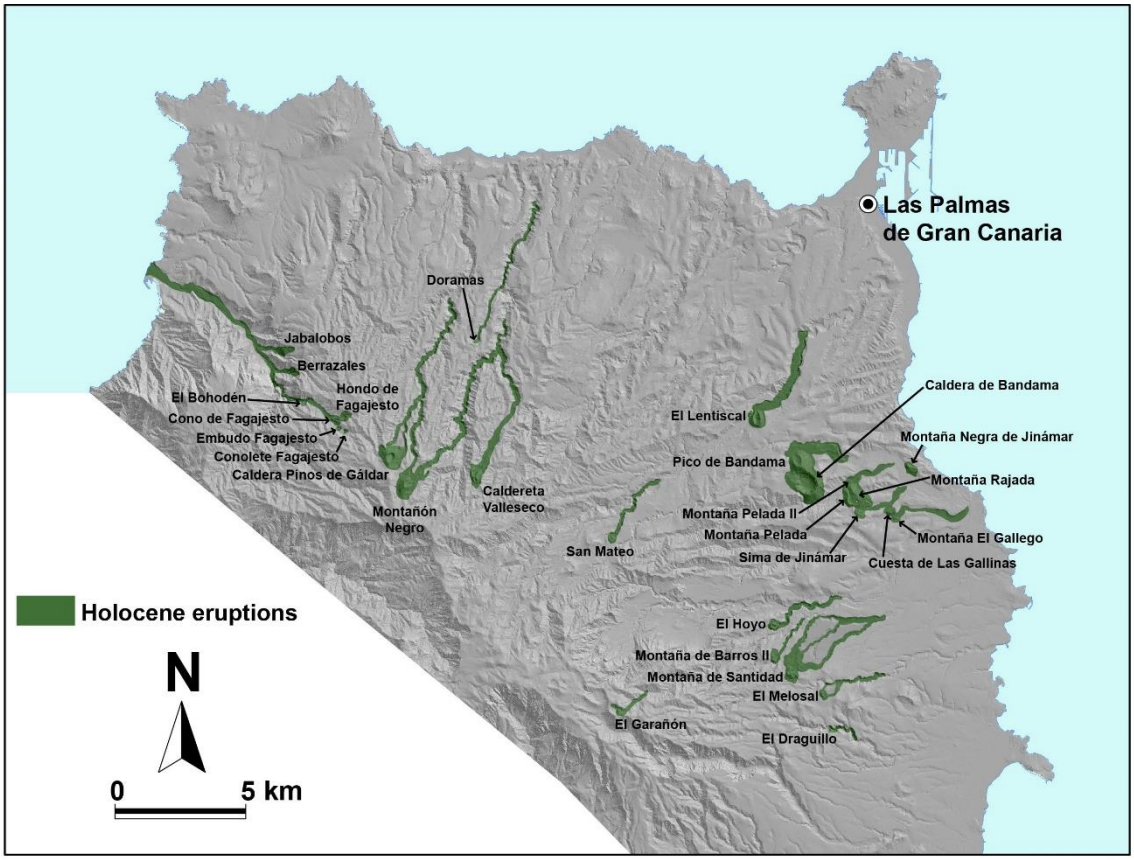

Figure 3.3. Location map of the Holocene volcanic activity (Rodríguez González, 2009).

From all Holocene volcanic eruptions in Gran Canaria, this work focuses on the most recent: Pico de Bandama eruption, dated 1970 ± 70 years ago (prehistoric times). It was dated using carbon 14 (^{14}C) radiometric techniques which organic material was obtained from plant samples. These were buried and incinerated by lava flows. Pico de Bandama eruption was located in Santa Brígida municipality. More specifically the volcanic building grown on northern slope of a divide known as Lomo de la Atalaya, and it intersects with Los Hoyos valley bottom (Fig. 3.4 A). This eruption was probably the most complex of all Holocene volcanic activity because it evolved from an effusive strombolian nature to a phreato-strombolian, much more explosive, which ended up creating a crater to south of the first unit and where another cone had previously been formed (Hansen et al., 2008). However, work is focus on Pico de Bandama and lava flow coming from it.

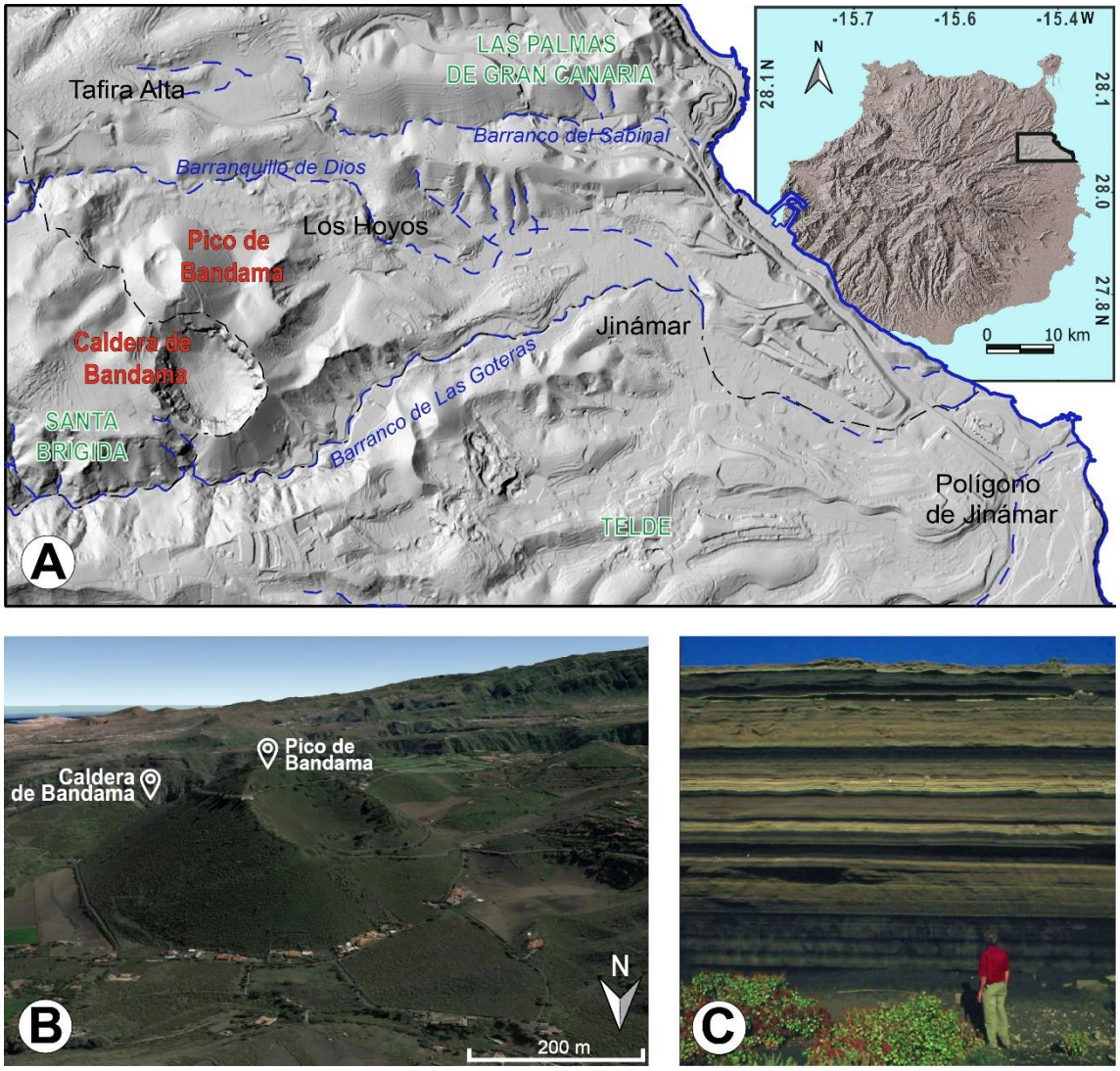

Figure 3.4. A) Location map of Bandama with municipal boundaries and principal ravines; B) Pico de Bandama building 3D view (taken from Google Earth); C) stratigraphic sequence observed 1 km south of the emission center (Hansen Machín et al., 2008).

Pico de Bandama constitutes the most outstanding topographic accident and the best landscape watchtower of the Gran Canaria northeast quadrant (Hansen et al., 2008). This volcanic building has a conical morphology, with mean depth crater of approximately 117 meters, in the shape of a horseshoe, symmetrical, little dismantled and open towards NNO (Fig. 3.4 B). Even so craters open to NE normally, by trade winds dominant influence that drags pyroclastic material from emission centers to SW. it is an accumulation of lapilli and slag. This one is more remarkable in crater edges, around emitting center. Also, a geological cut can be visualized on southern flank, where strata combined of pyroclastic flows (brown and cream) and lapilli's black layers can be distinguished (Fig. 3.4 C). this is another evidence of explosive mechanisms, in addition to fall pyroclastic mantle, whose horizontal dispersion area according to studies by

Rodríguez-González (2009) covers an area about $7{,}955{,}831\ m^2$ including a Santa Brígida and Telde good part.

There is a great lava flow from crater inside that subsequently flood the ravine channel called "Barranquillo de Dios" whose morphology is given by lateral slopes. Pico de Bandama Lava formed terraces at roof and they emphasize erratic blocks that have been transported by the own flow from crater opening. Besides, formation of mounds by gases scape on a scoriaceous surface are also observed.

Finally, descriptions make by observations during the fieldwork, as well as data interpretation they are fundamental factors since it gives way for a morphometric quantification in detail. It is obtained erupted material volumes, affected surfaces, lava viscosity, emission rate and topography. They allow estimating future eruption characteristics. It is especially dangerous if a lava tube is formed because it could allow to travel farther. In this case, a phreato-magmatic eruption is not ruled out, but probability is lower due to Gran Canaria actual low phreatic levels caused by human overexploitation.

4. VOLCANIC MORPHOLOGY: PALEO-GEOMORPHOLOGICAL AND TOPOGRAPHIC RECONSTRUCTION

Any volcanic relief is given by its morphological characteristics, where are identified volcanic cones, lava fields and pyroclastic mantles. These elements constitute the so-called volcanic units. For its description, geomorphology was used. It is responsible for studying an interest topography, in such a way that it recognizes earth's surface state, looking for causes that have brought it there. In this section, using GIS software, it is easier to know the relief evolution from a pre-eruption state to a post-eruption state. Processes that have modeled it over time can be discovered. That is the paleo-geomorphological reconstructions goal. Besides is essential to have knowledge about the lithostratigraphic units involved, specifically at Pico de Bandama eruption since nature of these yields very useful clues.

4.1. Topographic reconstruction

A topographic reconstruction consists in returning a certain land elevation to a possible condition that it had previously had. This is thanks to an intense fieldwork where it is doing present topographic units recognition and identification. Pico de Bandama volcanic building description and its main lava flow is a role entrusted to the SIG. However, lava flow emitted is the main volcanic unit of this work. Caldera de Bandama is the result of a phreatomagmatic eruption (see section 3.2) so the material comes out in the form of pyroclastic flow. On the other hand, Pico de Bandama building is necessary to determine approximately eruption thickness. Its only interest lies in complementing the lava flow study.

Reconstruction first step is to make a present Pico de Bandama geological map (Figure 4.1) where pyroclastic mantle extension, volcanic complex structure and lava flow coverage area are visualized. It can be observed how Bandama eruption emitted great amount of pyroclastic material that was transported by predominate winds to south and south-east. To achieve these results, it digitizes vector polygons characterized by attributes of the units in question above a Digital Elevation Model (DEM) by means of field observations. Given that it is an event that took place more than a thousand years ago, a slight dismantling by external geological agents is expected.

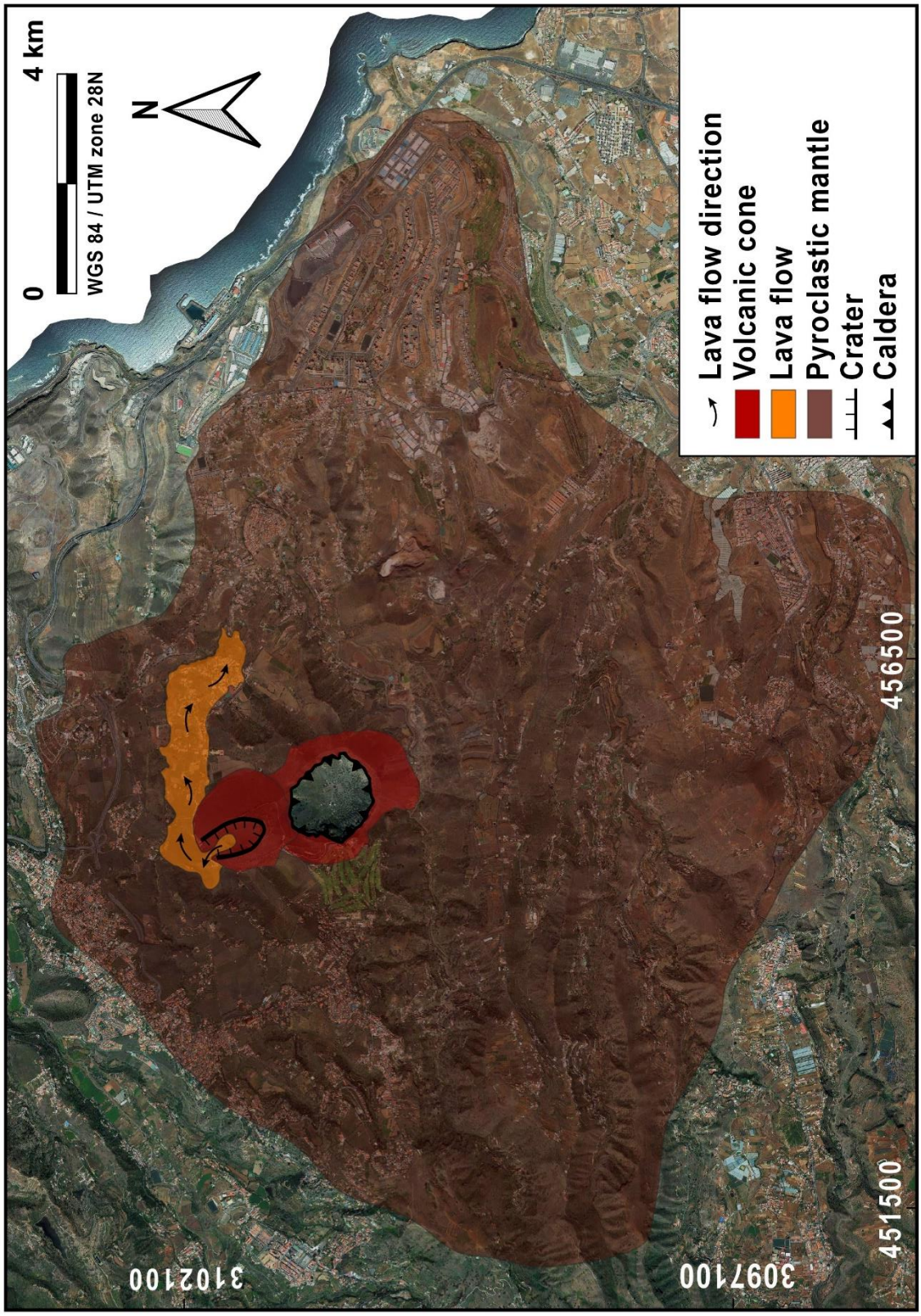

Figure 4.1. Geological map focused on Bandama volcanic units combined with orthophoto.

The lava flow and cone are digitized structures shed information on their surfaces. In addition, when it is combined with the DEM raster, data are also obtained on elevation, crater depth, or slopes as indicated in table 4.1, where some of these morphometric parameters have been compiled. They constitute fundamental data with which to know in detail the topography subject to study. They also are allowed to develop modeling, as well as the simulation of lava flows, which will be discussed later.

Table 4.1. Morphometric parameters and derivatives of Pico Bandama cone.

	Parameter	**Pico de Bandama**
Crater	Maximum edge elevation (m)	571
	Major axis (m)	563
	Minor axis (m)	306
	Eccentricity	0,8
	Major axis azimuth (°)	338
	Depth (m)	117
Cone	Major axis (m)	955
	Minor axis (m)	915
	Eccentricity	0,3
	Major axis azimuth (°)	324
	Cone height (m)	206
	Volume (m^3)	46951900
	Base area (m^2)	655366
	Basement lope (°)	
	Median	30
	Mean	29
	Minimum	0
	Maximum	46
	Standard deviation	6

The lava flow is studied by profiles approximately perpendicular to its longitudinal displacement, which is a digitized line on lava flow polygon. This vector analysis provides data about length, flow channel width and other data such as elevation at each point of said length (Table 4.2).

Table 4.2. Morphometric parameters and derivatives of Pico Bandama lava flow obtained by processing of 26 profiles or cross sections.

Parameter	**Pico de Bandama lava flow**
Length (m)	2586
Area (m^2)	852620
Volume (m^3)	10901200
channel width (m)	From 26 profiles
Median	346
Mean	331
Minimum	171
Maximum	504
Standard deviation	95
Thickness (m)	From 26 profiles
Median	14
Mean	14
Minimum	3
Maximum	26
Standard deviation	6
Lava flow base slope (°)	From 26 profiles
Median	5
Mean	6
Minimum	3
Maximum	12
Standard deviation	2

From this map, it is proceeding with Pico de Bandama land relief geomorphological reconstruction by altering contour lines manually in GIS software. Topography is molded conscientiously, taking into account that before the eruption there should have been a more uniform relief (no volcanic cone, no caldera), a ravine with lava filling absence and erosion equivalent to 1970 ± 70 years of rainfall (see section 3.2). Contour lines movement is not usually done all at once because like in sculpture arts, hands go through the surface in different reconstruction phases. First, the actual units are eliminated and curves are repositioned to obtain pre-eruption surface. Then, the holes created by erosion can be intuited by comparing the present surface with pre-eruption surface, so it is possible to fill them. At the end, it is also possible to get approximate Post-eruption surface. When the lava was unbroken, without ravine incision.

It should be noted that it is possible to start from contour lines contained in present-day digital maps or based on historical maps. However, latter have a somewhat more laborious methodology for scanning, georeferencing (involves control points definition in coordinate system) vectorization and contour lines correction.

Finally, with modified topography, computational processes are executed that allow software to transform topographic maps (vector) to DEMs (raster) and these to Shadow Models. Visually, the change it can be observed, relative to pre-eruption topography and the original one (Fig. 4.1). It emphasizes above all cone elevation on slope and ravine filling by lava flow.

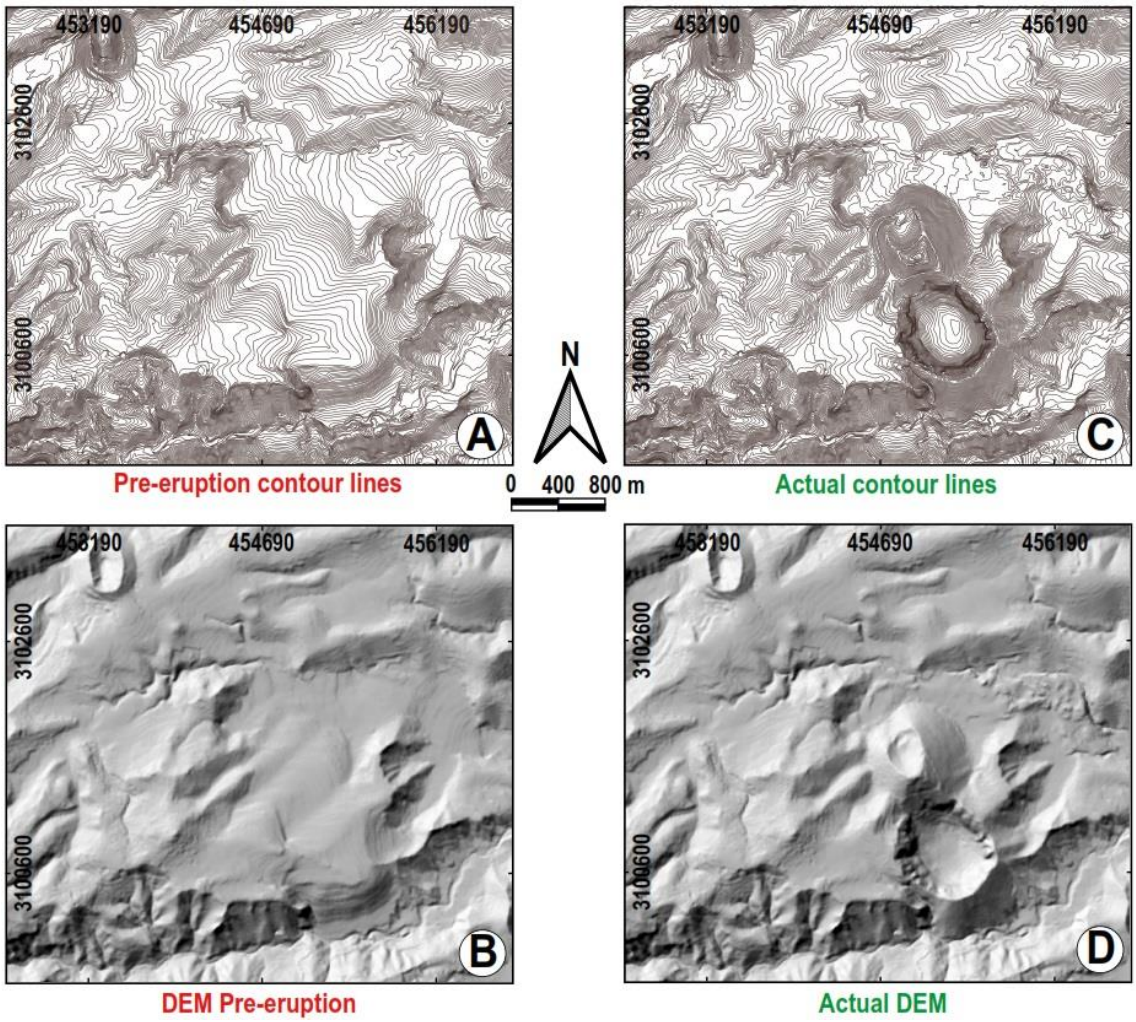

Figure 4.2. Comparison between Pico de Bandama pre (left) and post-eruption geomorphology. Starting from the current topography represented in contour lines (C), the relief prior to the eruption (A) is reconstructed. With these two maps an interpolation algorithm is executed to generate its DEMs.

4.2. Geomorphological reconstruction of Pico de Bandama

Pico de Bandama paleo-geomorphological and topographic reconstruction results provide the necessary information to know states that land relief has suffered. In Pico de Bandama case, like any volcanic eruption, its activity began with fissure opening in the terrain. Magma broke through the weakest and least resistant areas, so emission center was located in the lower part of one reconstructed paleo-ravine slope. Lava flow was advancing from crater, fell to the ravine bottom and flowed through it, filling its channel. Figure 4.3 shows different topographic profiles where it can observe land surface appearance. First, a pre-eruption state (Fig. 4.3 A), where the erosion of water has acted by shaping ravine over millennia since the typical smooth slopes U-shape is observed. Then, channel flooding by Pico de Bandama lava flow (Fig. 4.3 B) modifies the topography since what was once ravine bottom, has become a watershed. Therefore, ravine that previously had only one axis, now has two parallels (Fig. 4.3 C), one of them (right) being the present-day Barranquillo de Dios.

These two new ravine axes have a morphology very different from the one that existed previously. Surface rejuvenation by Pico de Bandama eruption, implies that external geological agents start from scratch to erode the new relief. As can be seen in figure 4.3 C, water impinges on lava flow sides, which in turn they are the lower parts, but that doesn't mean softer material. Water has could penetrate better through Barranquillo de Dios than through its parallel axis. It can be observed comparing post-eruption surface and the current one. Water flow wear has formed a ravine with steep slopes, a V-shaped profile and very fitted. Nowadays it is observed how water flow has eroded substrate below lava flow contact level (Fig. 4.3 C and 4.4). The parallel axis, on the other hand, contains pyroclasts and slag from lava flow, harder material that is difficult to erode, which is why it has hardly been affected.

Cutting and filling analysis in GIS software by comparing DEMs, it is possible to collect volumetric data (tables 4.1 and 4.2). The eruption total volume (V_O) is given by the overlaying between post-eruption and pre-eruption results. At the same time, the difference between present-day and pre-eruption surfaces give actual volume that it is conserved from eruption materials (V_A). Therefore, material evicted volume (V_D) is the difference between and ($V_D = V_O - V_A$; Rodríguez-González, 2009), which can be visualized in fieldwork (Fig. 4.4).

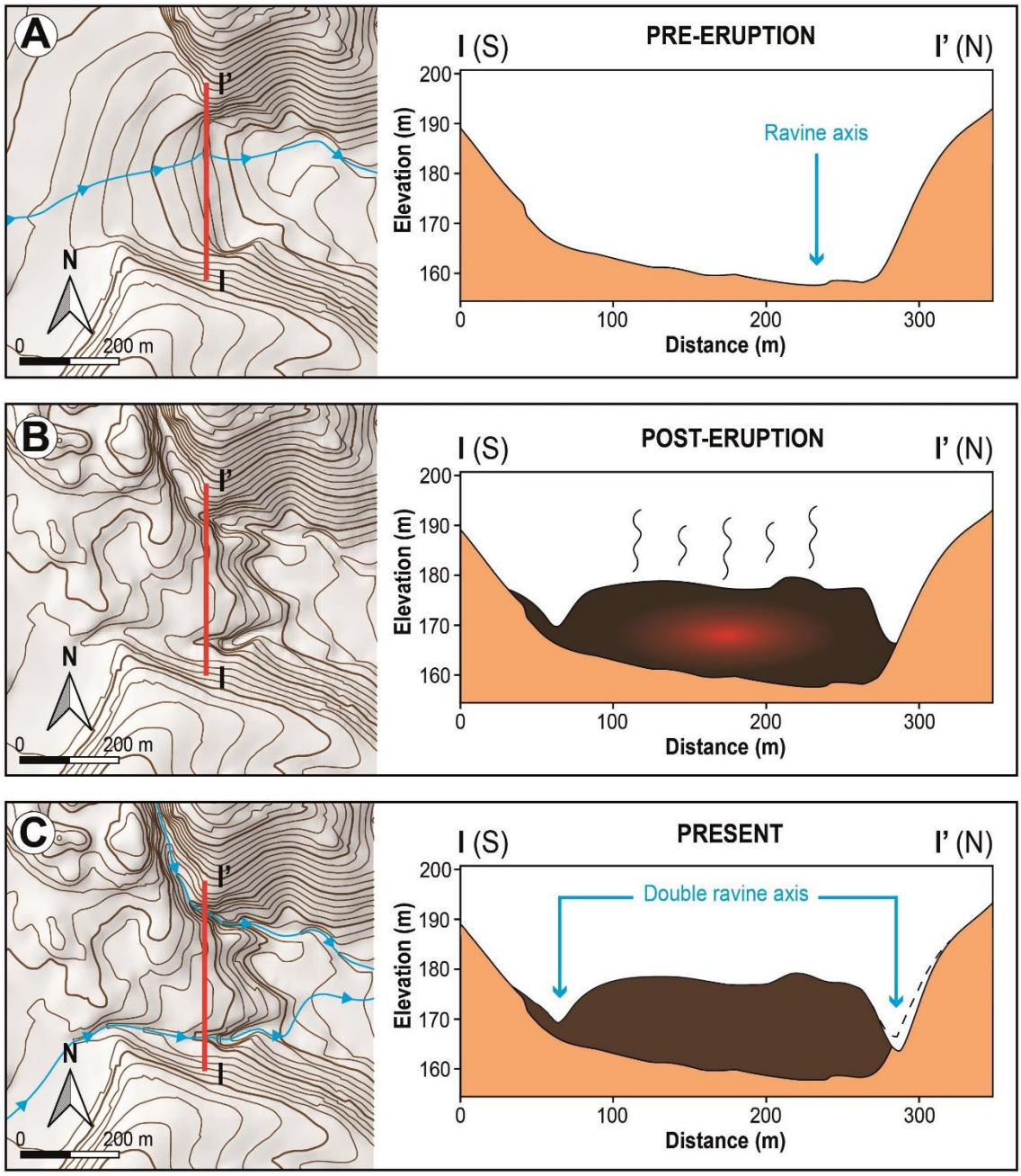

Figure 4.3. Geomorphological reconstruction of Pico Bandama lava flow at pre-, post-eruption and present-day times. A) Pre-eruption topographical reconstruction, showing ravine axis and direction, and a representative topographic profile; B) Post-eruption topographical reconstruction with a representative topographic profile showing channel filling by lava; C) Present-day contour lines showing the two channels formed. There is a line in the topographic profile that indicates material dismantled by water.

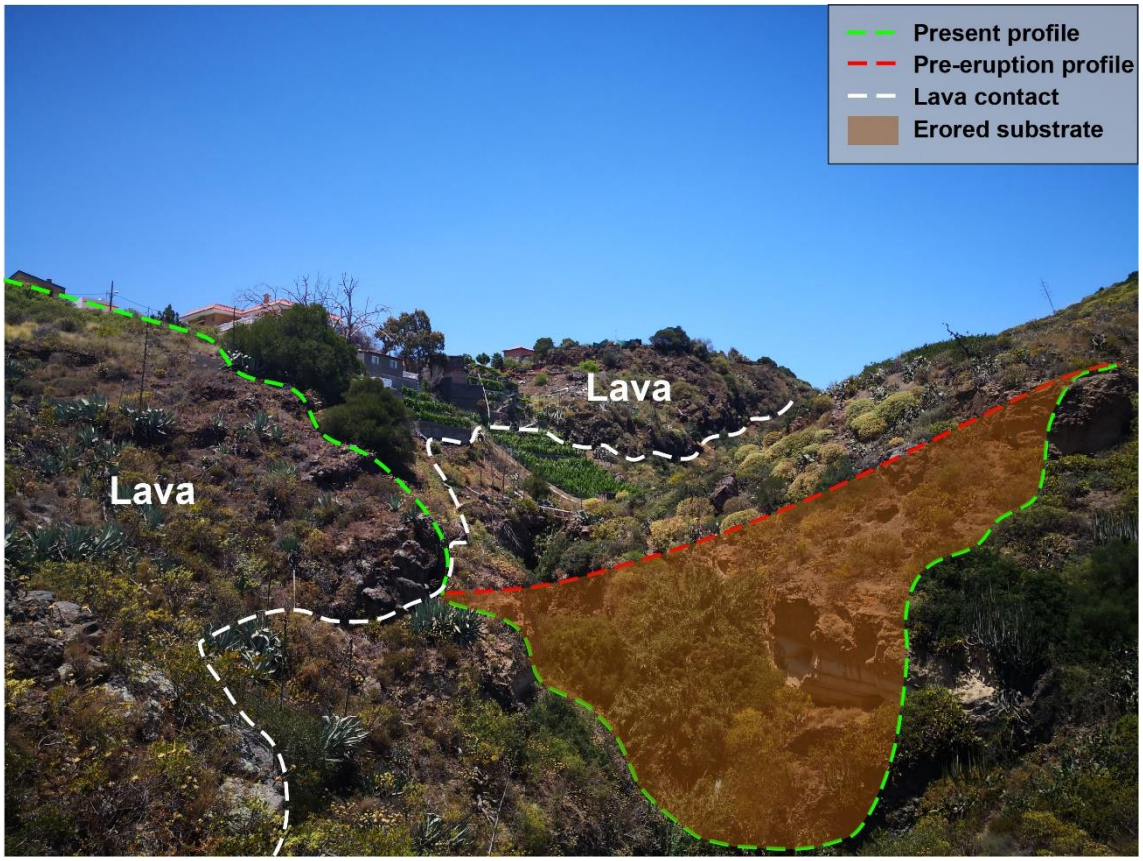

Figure 4.4. Field view of dismantling produced in lava flow lateral contact through "Barranquillo de Dios".

4.3. Digital Elevation Models quality

Throughout previous section, it was mentioned terms such as DEM and shadow models. In DEMs case, they are represented altimetry data by contour lines interpolation, generally. Interpolation algorithms can give different results to reality. Due to these models are essential in a morphometric study, a quality check is necessary. It seeks a computational processes optimization, with a reaching acceptable error margins. Quality evaluation is carried out by means of three points: contour lines check with model z-values, comparing volumes and comparing slopes.

In this case, GIS software has interpolated using Inverse Distance Method (IDW) from contour lines. They are configured by abundant points located with some regularity. This method is highly recommended for such point distributions, so it is accepted as good in this morphometric study.

On the other hand, resolution or pixel size in models is a matter to be taken into account. There is no linear correlation between resolution and the quality, in other words, a higher resolution, it does not always entail a better quality. Thus, if the resolution is too

high (smaller pixel size), computer processes to elaborate each task would take too long. Efficiency at work is lost. And if resolution is too low (larger pixels), very different data of contiguous cells could be averaged generating cumulative errors. According to studies by Rodríguez-González (2009), DEM resolution best suited to the $1:5000$ work scale is $5x5\ m$. However, this fact will be tested in later sections through studies with Pico de Bandama eruption.

5. PETROLOGICAL-GEOCHEMICAL DESCRIPTION OF PICO DE BANDAMA LAVA FLOW

5.1. Lava petrology

In general, the Holocene lava flows that have occurred in Gran Canaria shows a very characteristic petrography. Everything has a porphyritic main texture (large crystals) with clinopyroxene and olivine phenocrysts as the most remarkable minerals and an aphanitic texture secondary in the matrix. Olivine crystals constitute a fresh and greenish macrocrystals mineral phase that have formed without disturbances. Its presence standing out above others and whose content varies between three and 30% in the rock. On the other hand, are also a mineral phase well represented in lava, appearing like phenocrysts, microfencrystals and microcrystals forms in the matrix. From petrographic characteristics, different clinopyroxenes phenocrystals have been divided into three categories: (1) brown phenocrysts with normal zoning, (2) unfenced green phenocrysts and (3) zoned phenocrysts with green nuclei and brown edges. Each of these classes indicates the magmatic chamber state at the eruption time. Consequently, offers a clue about eruption behavior.

The Pico de Bandama lava flow case, all samples indicate that it is a lava with more than 90% its volume composed by crystals (holocrystalline). It is class 3 clinopyroxene phenocrysts that characterize Pico de Bandama lava. There are also feldspatoids (nepheline), Fe-Ti oxides and plagioclase in the aphanitic texture. Regarding vesicularity, it doesn't exceed 4%. This a very important data for data inserting in lava flows simulations because it is used in the volume of dense rock equivalent (DRE) determination that consists in material volume expelled in eruption by applying a correction factor that takes into account rock hollow volume (pores) in order to obtain solid matter amount.

There is hardly any textural and/or paragenetic variability in lava samples. It only highlight regions with different types in clinopyroxenes that have connotations in the mechanisms of magmatic differentiation (Rodríguez González, 2009).

5.2. Lava geochemistry

Geochemical data reveal that Holocene lavas are very fresh and homogeneous both from a compositional, mineralogical and textural point of view. It demonstrates that fractional crystallization processes and the magmas mixture are not the dominant ones.

This includes the Pico de Bandama eruption, although clinopyroxenes petrographic analyzes offer information about a weak fractionation in magmatic chamber. This process allowed green clinopyroxene crystal development. A subsequent new magma injection originated growth of a less evolved brown mantle around the nucleus, just before the eruption. On the other hand, macrofenocrystals olivine chemistry of olivine is rich in magnesium whereas the microfenocrystals are richer in iron.

The Pico de Bandama lavas are alkaline. It is a basic composition due to a low silica content. In addition, high content in olivine, indicates that its rock type classification corresponds to a basanite.

6. MODELING LAVA FLOWS

The lava flow nature, type of composition and the surface where it flows are aspects to be considered before modeling lava flows. The lava flows behavior or their way to flow in the natural environment are the most interests in these studies. Related to this, the degree of volcanic eruptions violence is inversely proportional to the material size that is expelled. Therefore, if materials come out quietly, they run through ground like a lava flow.

The lava is a special fluid type called Bingham (Fig. 6.1 A). This class of fluids are non-Newtonian and their dynamics work based on cohesion between molecules in molten material and also it depends on gravity, either allow it to advance in favor of slope. If we had a lava cube, this cohesion wouldn't hold top fraction and collapse, spilling out to the sides, until lava reaches a certain thickness more stable (Carracedo, 2008). The lateral expansion by tendency to balance between height and width implies that a flow extends to width until reaching a certain measure. This fact is independent to free ground extension on which lava flow it expands. On the other hand, there are limits in the fluid where the lava flow shear strain isn't sufficient to allow its advance. These are lava boundary conditions. Hence, if the limit is the floor, there is no displacement, due to friction. It also happens on the sides, forming the characteristic lateral lips or “leveès” (Rielo, 2002).

While emission center continues to expel molten material, a lava flow may continue to advance along the topography, due to said material pushes the one in front of it. This push generates the total lava flow advance. When the supply ceases, lava flow reaches an equilibrium and begins to cool and crystallize. Immediately, the lava achieves a resistance to movement that stops it definitively, even if it is located on a slope (Carracedo, 2008).

6.1. Effusive eruptions and physical-chemical parameters of the lava flows

The most decisive factor in the volcanic eruption behavior is magma composition that will come out in lava form. For Pico de Bandama eruption, lava flow is basaltic, concretely of basaitic composition (section 5), which is typical of effusive eruptions.

The characteristics of lava depend on many intrinsic factors. These would be: crystallization conditions, as well as their shape, aspect ratio (horizontal

thickness/extension), surface structure and, the nature. These must be introduced in the corresponding lava flow simulation models, and include composition, temperature, viscosity, crystal content and gas content. Some derive directly from magmas, and remain invariant, but others are variable and can change irreversibly. When a lava comes in contact with atmosphere, it begins to cool. Thus its temperature goes down continuously, while volatiles escape, crystals increase both in number and size, and flow viscosity and resistance increase until the movement stops. Its speed is also taken into account in models, although indirect extent since it depends on the eruptive rate (volume emitted per unit of time), in addition to the slope through which it flows and the viscosity of the lava itself.

6.2. Lava flows classification

The Pico de Bandama eruption was effusive, as explained in previous sections. Still that doesn't mean that there is a single lava flow type since several different kinds of subaerial flows can be originated, cataloged according to surface aspect. However, general classification includes other types, which are listed in table 6.1.

Table 6.1. Lava types general classification according to the environment and appearance of its surface. It's presented international and Spanish nomenclature.

Environment	International Nomenclature	Spanish Nomenclature
Submarine	Pillow lava	Lava almohadillada
Subaerial	Pahoehoe	Lava lisa o cordada
	a'a	Lava rugosa o malpaís
	Blocky lava	Lava en bloques

- **Pahoehoe.** They present smooth or folded surfaces in the form of strings, hence their name in Spanish ("lava cordada"). If advance is observed live, formation of fingers that move very slowly (Fig. 6.1 A) stands out. When one finger is fixed others move on it or contour it, generating the lava flow front general advance. Finally, thin layers or units of lava flow remain. In the case of sharp slopes, thin crust is folded and twisted, and on flat surfaces, when cooled it is completely smooth.
- **A'a.** They are characterized by having a scoriaceous surface, very fractured in irregular and loose fragments that make it very difficult to walk on them. If we observe its movement live, we would see a single stream (Fig. 6.1 B) whose working resembles that of a conveyor belt. It consists that slope of the lava flow front is continuously collapsing since the base remains motionless while the rest of it continues to advance and surpasses it. These flows tend to be channeled by temperature differences between the hottest stream and the coldest laterals

forming leveès. Lava flow morphology in blocks (Blocky lava) is similar to a'a, only that they are own of more explosive eruptions.

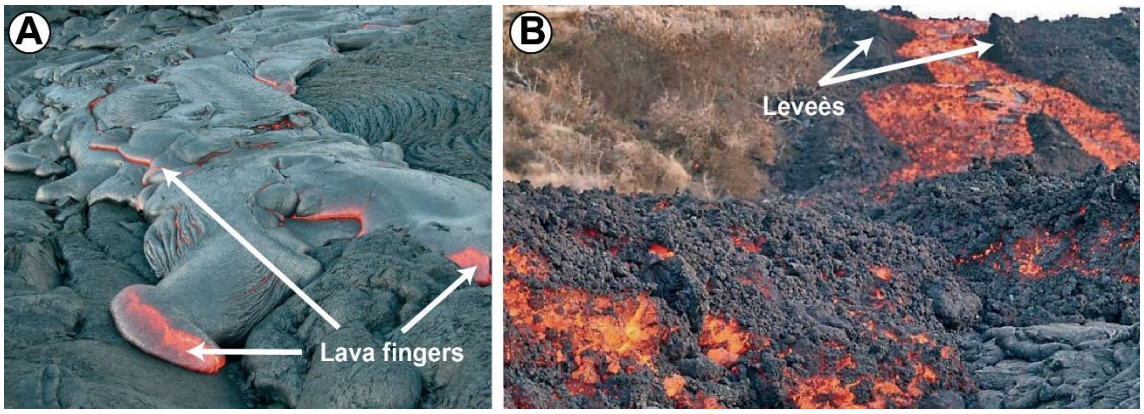

Figure 6.1. Different types of lava flows: Pahoehoe moves through fingerings (A) and a'a flows as a direct current (B). Both from the Puu'Oo volcano, Kiauea, Hawaii (Modified from Carracedo, 2008).

The change pahoehoe morphologies to a'a is frequent within the same lava flow. If the flow speed increases, to achieve a flow rate about 10 times higher, mentioned transformation occurs. If the viscosity increases this processes also occurs. Besides topography influences either positively or negatively to change to a'a lava flow type.

6.3. Lava flows path modeling methods

Analyzing how a lava flow does it move is quite complex due to its characteristics that define the nature of the same. These phenomena numerical modeling isn't far behind in terms of complexity because it is necessary discretization of a Bingham fluid equations that describe it. In addition, its motion motor is viscous thrust influenced by gravity. These are factors introduced in the algorithms. On the other hand, determination of the parameters that govern equations mentioned aren't simple to obtain, since laboratory experimentation is necessary and recourse to certain resources.

These difficulties set has required the development of different methods to lava flows numerical modeling, in order to better understand movement of these. They have been classified into two main types:

- **Deterministic models.** They are based on transport theory discretization from differential equations that describe mass conservation, momentum and energy balance. The resulting equations (Navier-Stokes equations) are non-linear, and since they don't have boundary conditions, free surface information and energy losses, complicate obtaining the results. Thus, several approaches to Bingham fluid theory

are applied. Modeling is more viable by simplifying equations that describe the phenomenon. In this work, it was opted for the model offered by the Q-LavHA plugin, the *FLOWGO* model by Harris and Rowland (2001), of the numerous models that have been proposed over the years, such as, for example, *FLOWFRONT* by Young and Wadge (1990) or *LavaSIM* by Hidaka et al. (2005).

FLOWGO. Autoadaptive numerical model for a lava flowing inside a lava channel. The models basis is lava speed estimation as a Bingham fluid within a channel. During each step of the simulation, heat losses and gains are calculated to determine their effects on lava rheology (fluid dynamics). Lava flow will stop when it reaches the solidus temperature or reaches zero speed. This model needs a physic-chemical parameters diversity to work (Appendix I) and it was validated in a lava field in Mauna Loa, Hawaii (Harris and Rowland, 2001).

- **Probabilistic models.** They are based on the fact that topography is main factor to control the lava flow advance. These models are able to identify areas potentially invaded by lava and calculate the probability that a pixel on a DEM will be flooded. It is taken into account that it is impossible to flood pixels higher than the starting point (ascending slope) and not too deep ones. In contrast to deterministic ones, these don't suppose a great load of computational processing. Once again, it was opted to take advantage of the models implemented in Q-LavHA:

Maximum Length (L_{max}). It defines a maximum length (m) to where the lava can flow, understanding it as the distance traveled by lava flow line, not the entire lava flow distance. This distance can easily be estimated by studying maximum length reached by historical lava flows of the volcano studied (Mossoux et al., 2017). The length data that is entered into program must be multiplied by an empirically established correction factor (Appendix II).

Decreasing Probability. Assumes that probability that a lava flow reaches a certain length can be expressed with a decreasing cumulative probability density function, following a normal distribution. So, it ponders pixel flooding probability by means of average length and standard deviation of the historical lava flows of a volcano or of a same period (Appendix III), as in this work, which is considered the Holocene volcanism in Gran Canaria (Mossoux et al., 2017).

However, it is highlight existence of two recently published and very promising models in the volcanic hazard research to complement current studies. Firstly, the model *MrLavaLoba* (Vitturi and Tarquini, 2018) functioning is based on a

probabilistic law influenced by steepest slope direction. Informatic's processes try to guess the most likely pixels to be flooded by a lava flows and the thickness it would reach. It is similar to the previous L_{max} model, but with the possibility of application to pahoehoe lavas. Secondly, *MULTIFLOW* (Richardson and Karlstrom, 2019), intends to go beyond a single flow line since, there is interaction between flow paths and topography through which it flows. Topography is usually very irregular, causing ramifications in the "main" channel. Therefore, an algorithm is included that quantifies the most important topographical lengths to influence lava flow paths. In addition, the threshold function that limits lava flow extension according to its thickness was implemented.

7. Q-LAVHA AND ITS INTEGRATION TO SIMULATION MODELS

Q-LavHA (Quantum-Lava Hazard Assessment) is a free plugin created to work in an open source and multiplatform Geographical Information System environment, distributed through "www.qgis.org". Once installed, it is incorporated in QGIS toolbar or complements menu, through which you can access it (Mossoux et al., 2016). Its purpose is to simulate the flood probability of a lava flow a'a channeled from one or several emission centers regularly distributed in a DEM using an iterative approach. Based on the options set by the user, this plugin calculates a predefined lava flow lines number (iterations) that are then combined based on the simulation parameters activated to express the probability that a pixel will be flooded by lava.

On the other hand, it is able to combine existing probabilistic and deterministic models and proposes some improvements to calculate the probability of lava flow spatial propagation and final length (Mossoux et al., 2017). This function allows users to evaluate, compare and finally select the most convenient, based on available data and knowledge about lava flows that are modeled.

When accessing to plugin interface, three different sections are presented, all dedicated to parameters introduction, which can be saved during the simulation or import the previous ones:

1. ***"Input files":*** Includes DEM insertion (raster layer) that constitutes topographic base where simulated lava is supported. Also, an option to calculate index fitness based on a real lava flow raster and a button where it must indicate output file location. Both raster layers: DEM and actual lava flow are automatically converted to a ".asc" format required by Q-LavHA.
2. ***"Vent location":*** It has options to define emission center location and eruptive source type, which can be a specific point, a linear fissure or a surface. First two types allow the user to simulate a lava flow emitted from a well-defined point or an eruptive fissure, respectively. Surface option allows to simulate multiple eruption scenarios in a probable eruption area. Coordinates for these last two situations can be inserted manually or automatically from an existing vector file (shapefile) (Mossoux et al., 2016). Another option is probability density function map (PDF) selection. It provides information about different emission center locations occurrence probability, that map is chosen and the minimum susceptibility value is introduced for simulation. For linear fissures cases, and

surfaces, a distance should be defined between emission centers points of lava flows.

3. ***"Lava flow parameters":*** Lava flow data related to propagation, length restrictions, iteration number, and minimum (H_c) and medium (H_p) of the lava are entered here. Used to produce simulated lava flow probability raster. Only pixels with probabilities higher than thickness defined by the user are shown in a resulting file. In addition, there are two options to mark that enable analysis method of DEM at 16 pixels ("H_{16}") and the possibility of that flow lines advance taking steepest slope ("*Probability to the square*"). This options differs based on the model chosen for execution. Maximum length only needs one parameter, decreasing probability needs two and several physic-chemical FLOWGO (see section 6).

Once plugin run, code begin working. Models equations extract from a DEM, the pixels' elevation surrounding lava. According to the defined rules, one or several (maximum 8) surrounding pixels are selected where lava can start to propagate. For this, slope is taken into account because as explained in section 6, a lava behaves like a Bingham fluid and its flow go in favor of slope, and this is stipulated by models. Then, the probability that a pixel will be flooded is proportional to slope. If this is negative (ascending incline), the probability is zero and simulated flow stops. Nonetheless, if next pixel is at a much lower level (strong vertical wall) and constitutes a depression too deep to be overcome by correction factors considered, Q-LavHA expand scanning to 16 neighboring surrounding pixels (Fig. 7.1 A). If one of these 16 pixels doesn't meet requirement to continue the simulation, then simulated lava flow stops its spreading.

To determine next pixel will be flooded probability, it is important to take into account altitude at which the surface of the pixel is located. This verification is simple to understand: if difference between pixel elevation where the lava is and the next is positive, it will can continue filling and flow progresses, thus being able to overcome minor topographical obstacles. To make this possible, some correction factors are applied, considering lava minimum thickness (H_c) and its average (H_p). Latter allows filling deeper depressions that otherwise would have stopped simulation erroneously for numerical reasons (Fig. 7.1 B).

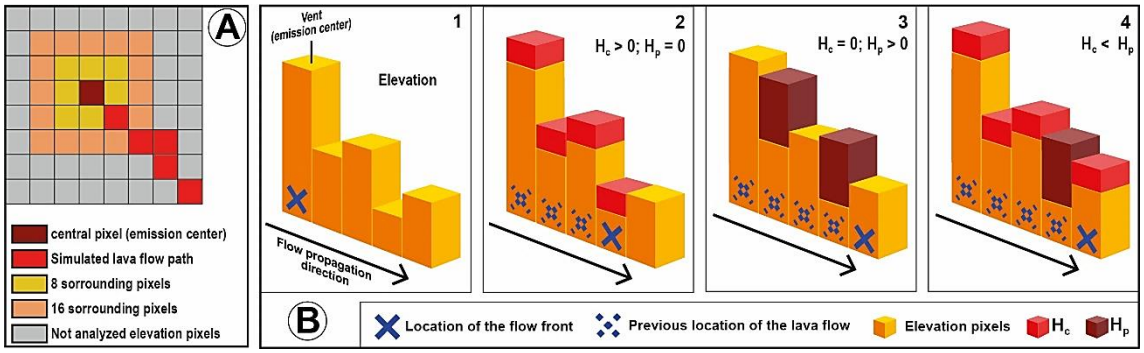

Figure 7.1. Conceptual visualization of the propagation of a simulated lava in Q-LavHA. It starts from a source pixel to the surrounding ones (A) and lava front advances taking into account the thickness correction factors when filling pixels at lower levels.

The output produced by Q-LavHA, expresses the probability that a pixel will be flooded by lava, and is presented in raster format ".asc" as a flood probability map which can be added to an active QGIS project. This probability covers an integration of all lava flow lines calculated from one or several eruptive points. Lines number is defined by iterations number that has been specified in Q-LavHA. Apart from raster layer, a text file (".txt") is simultaneously produced that includes a summary of both parameters used during the simulation and results, as well as values calculated for a fitness coefficient, called Fitness Index (*FI*). This coefficient makes it possible to evaluate simulated lava flow precision, comparing it with a real lava flow mapped. Overlap between them is interpreted by $FI_{True\ Positive}$ values that vary between 0 and 1. Besides, there are two additional parameters that represent overestimated areas ($FI_{False\ Positive}$) or underestimated ($FI_{False\ Negative}$). Sum between these three numbers must give 1 representing total modeled flow.

8. PICO DE BANDAMA LAVA FLOW SIMULATION ANALYSIS

Explaining either operation at algorithm level of the Q-LavHA plugin and basic principles of its three models implemented (L_{max}, *Decreasing Probability* and *FLOWGO*) are the philosophy behind lava flows modeling has been described previously (see sections 6 and 7). Next, results obtained in the Pico de Bandama lava flow simulation for these three models are presented. This work begins describing the first simulation tests performed with L_{max} model, since it is highly recommended if a determined person doesn't have enough knowledge about lava properties or simply it want to establish a first contact with Q-LavHA processes. In addition, interpretation and analysis of the results are presented through studies about data introduced performance, model's limitations and DEMs importance.

8.1. The influence of parameters used in the simulation models

When corresponding parameters get into Q-LavHA, the implication of them results variability must be known. So, the resulting lava flows can become very different from expected adaptation to a real lava. Although in a less significant way, with the same values each program execution will lead to different outputs.

The most important parameters in this analysis are those that limit lava flow propagation. They are about correction factors H_c and H_p already defined (see section 7). The simulation started from a point emission center (Pico de Bandama), whose mapped lava has been calculated a minimum thickness on 2 meters (H_c) and an average thickness on 14 meters (H_p). Lava flow trajectory was simulated over a surface with an average slope of 6º (see table 4.3). Then, the options "H_{16}" and "*Probability to the square*" was disabled at plugin because it only interests to study the simulated lava flows behavior under different thickness values. The result is shown in figure 8.1, where we can observe 4 different simulated lava flows made by the L_{max} model, from null values in figure 8.1A ($H_c = 0\ m;\ H_p = 0\ m$) up those obtained from the actual lava flow mapping in figure 8.1D ($H_c = 2\ m;\ H_p = 14\ m$), going through the combination between these values in figure 8.1B ($H_c = 0\ m;\ H_p = 14\ m$) and figure 8.1C ($H_c = 2\ m;\ H_p = 0\ m$).

In the case of figure 8.1A, the fact of defining null thickness values doesn't allow flow lines to propagate properly through the DEM, since lava front moves very limitedly through the pixels. Whenever a sufficiently severe depression or a relatively small obstacle is encountered, a flow line stops at that point. Therefore, a casting with high values of flood probability (more intense red) is achieved, where there is a succession of

pixels with little difference in height that is, in channel center. If only the average thickness is applied (Fig. 8.1B), a lava flow similar to the first one is obtained since this factor is theoretically useful when combined with the minimum one. The average thickness is greater than this, so it has greater involvement in the simulation processes, as can be seen in figure 8.1C. The first appreciable difference is lava extension, which is larger than in figure 8.1A, this implies that the front propagates better along DEM, flooding the ravine either in its deeper and flatter areas and across its channel. The maximum flood probability in the center is smaller than in figure 8.1A (dimmer red), because the probability is dividing by a greater pixel's number. On the other hand, the distance in a straight line between vent and front is shorter than the defined distance. This is opposite to the fact that none of the factors apply, which extends beyond.

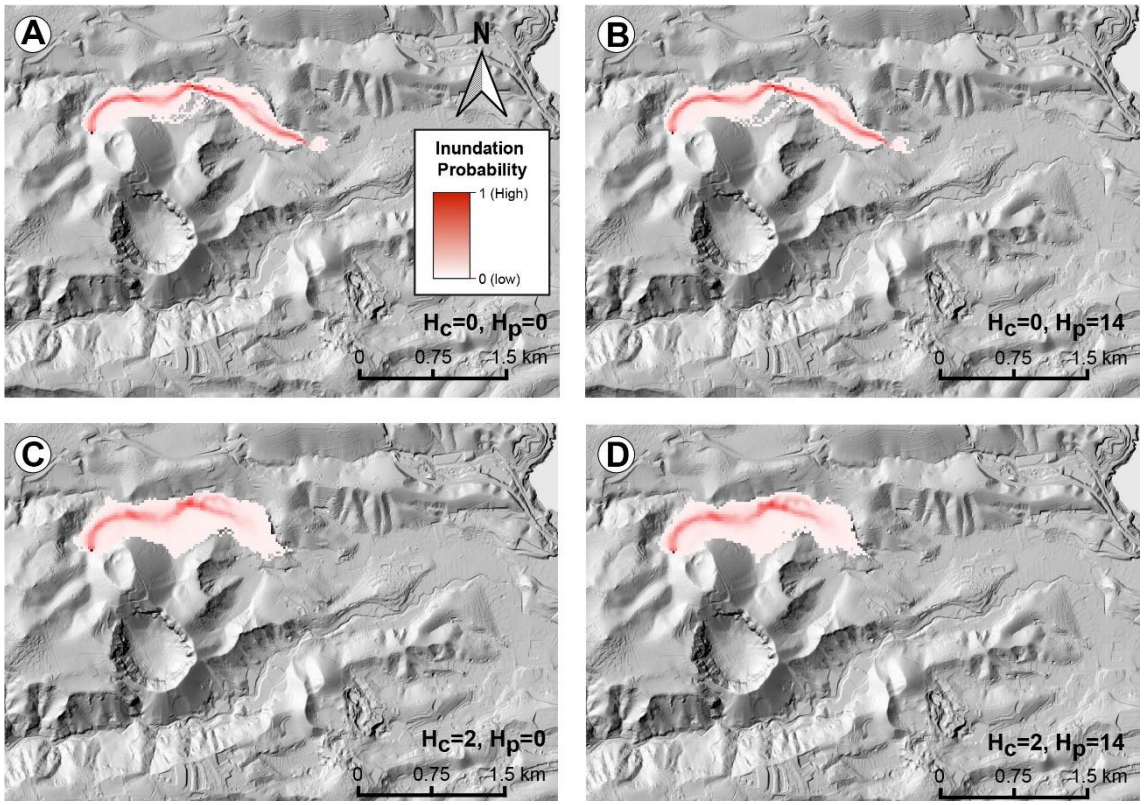

Figure 8.1. Results of lava flow simulations with different values of minimum and average thickness. "Probability to the square" and "H_{16}" options are disabled.

However, activating "*Probability to the square*" and "H_{16}" options that had not been previously enabled gives more optimized results. It obtains to a better approximation to Pico de Bandama lava flow (Fig. 8.2). On the one hand, the effect of channeling the lava in flatter areas is accentuated. The flood probability is concentrated in the channel center for all cases (Fig. 8.1A-D) and at the same time, the flow width narrows, especially remarkable in figure 8.1C and D. It was like being expected in reality because for mass conservation, lava volume that has not flooded laterally, allows the front to move farther,

coinciding better with the mapped lava. However, in simulations where null values are introduced or only H_p they also advance even more with respect to those obtained in figures 8.1 A and B respectively.

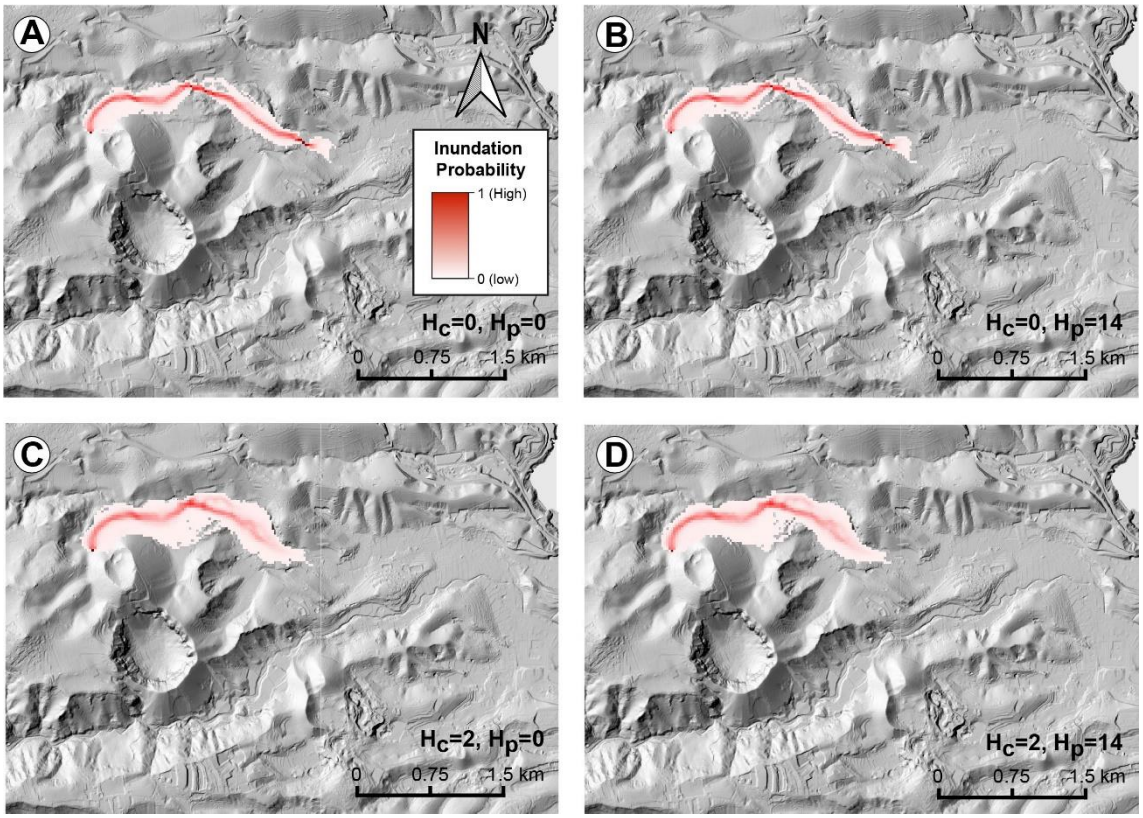

Figure 8.2. Results of lava flow simulations with different values of minimum and average thickness. "Probability to the square" and "H_{16}" options are enabled.

The lava thickness values are not only applicable to L_{max} model, but also to *Decreasing Probability* and *FLOWGO*. Consequently, very diverse results are could expect, although all of them tend to process digital topography to represent a determined lava flow. This implies the possibility of comparing results from each of them based on how the algorithm propagates the lava flow. In other words, how it considers the values of H_c and H_p in each pixel.

Figure 8.3 presents pixel's number affected by the flow lines advance, applying the three models of Q-LavHA, to visualize the propagation by combining the thickness values, as well as determining when it has been necessary to apply the 16 surrounding pixels search function, which gives continuity to simulated flow path: first with the minimum thickness (H_c, in blue), the average one (H_p, in green), the minimum one extended to the surrounding 16 pixels (H_{c16}, in yellow) and with the average thickness also extended to the surrounding 16 pixels (H_{p16}, in red). If this last criterion isn't met, the lava stops. In figure 8.3A and C almost all the lava flow is propagated by the minimum

thickness topographic correction, while figure 8.3B shows the need that the algorithm has had to resort more frequently to higher order corrections, especially beyond where real lava front is located. Also, it is worth noting the flow line's extensions that go far beyond the actual lava flow. As was discussed in section 6, *Decreasing Probability* model generates a flood probability map taking into account the average length and standard deviation of all Holocene eruptions. The mean length and standard deviation values were calculated at 3793 and 2702 m respectively. Consequently, a lava flow with a length up to three times greater than those resulting from the other two models has been generated.

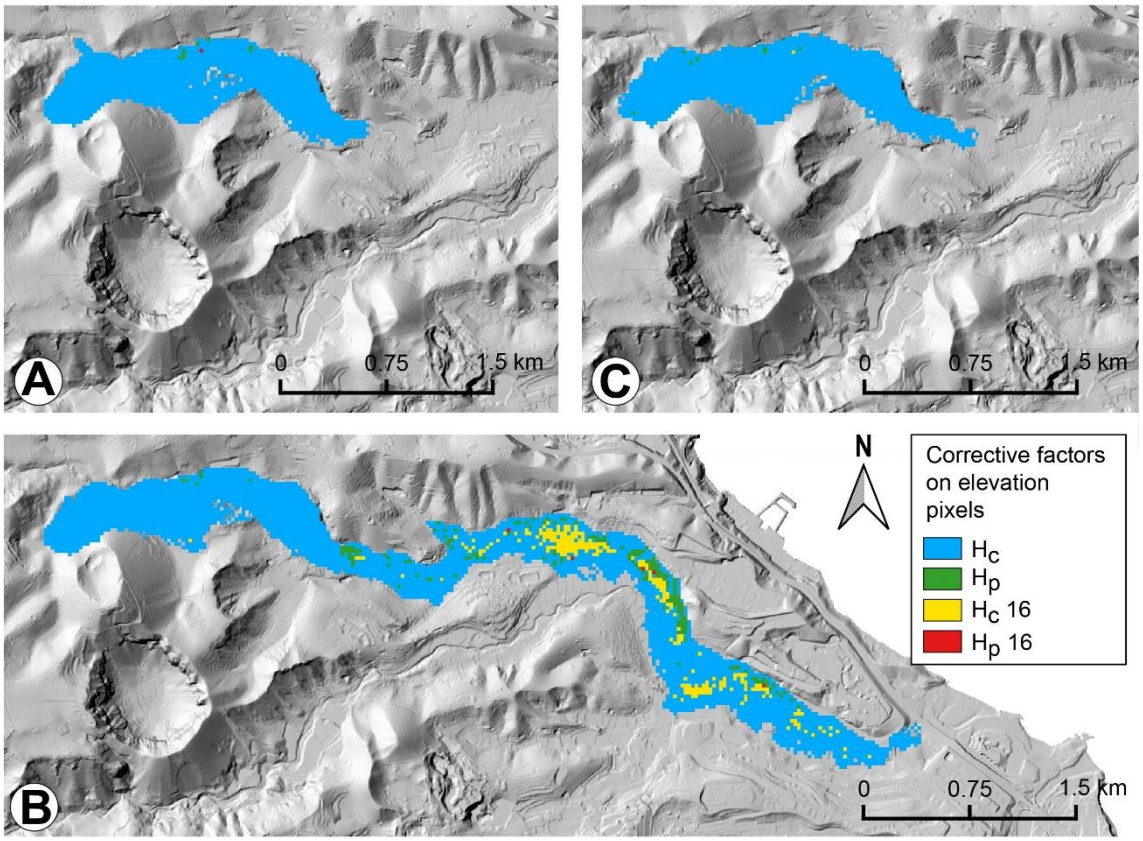

Figure 8.3. Visual representation of H_c, H_p values and H_{16} criteria in each pixel. These were applied in the simulation models: A) L_{max}, B) Decreasing Probability and C) FLOWGO.

Visually, it highlights which of the three applied models could be the most suitable for the Pico de Bandama lava flow simulation. However, analyzing the optimal simulation for each of them based on the value of H_c and FI (see section 7) is very convenient to better understand the lava flow behavior. Optimization occurs when a maximum FI is reached for a given H_c. Figure 8.4A shows result of collecting FI data for 20 simulations applying the L_{max} model and represented in a graph H_c versus FI. The minimum thickness with which the adequacy maximum value is reached with the overlapping FI (0.68) is 2 meters. On the right to graph, simulated lava flow is presented and where the maximum probability coincides perfectly with actual lava flow perimeter. On the other hand, an

optimal simulation is equally applicable to the *Decreasing Probability* or *FLOWGO* models, with a minimum thickness of 2 meters.

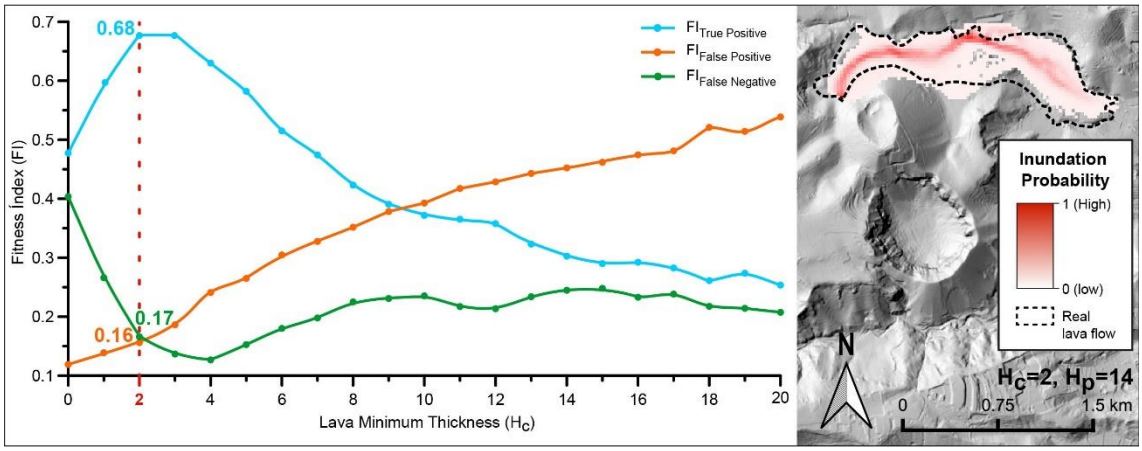

Figure 8.4. Optimal simulations with a H_c versus FI graph that indicates the processing made in the optimal simulation study for L_{max} model (A). Optimal simulated lava flows are also shown for Decreasing Probability (B) and FLOWGO (C).

8.2. Lava flow length limitations and its implication in simulation models

Which of the model's subject to study must be chosen for a volcanic terrain model development with as little uncertainty as possible? The key to answering this question is coincidence degree between real and simulated lava, or *FI* index (see section 7). So, results have to coincide with the cartography of Pico de Bandama eruption in the best way.

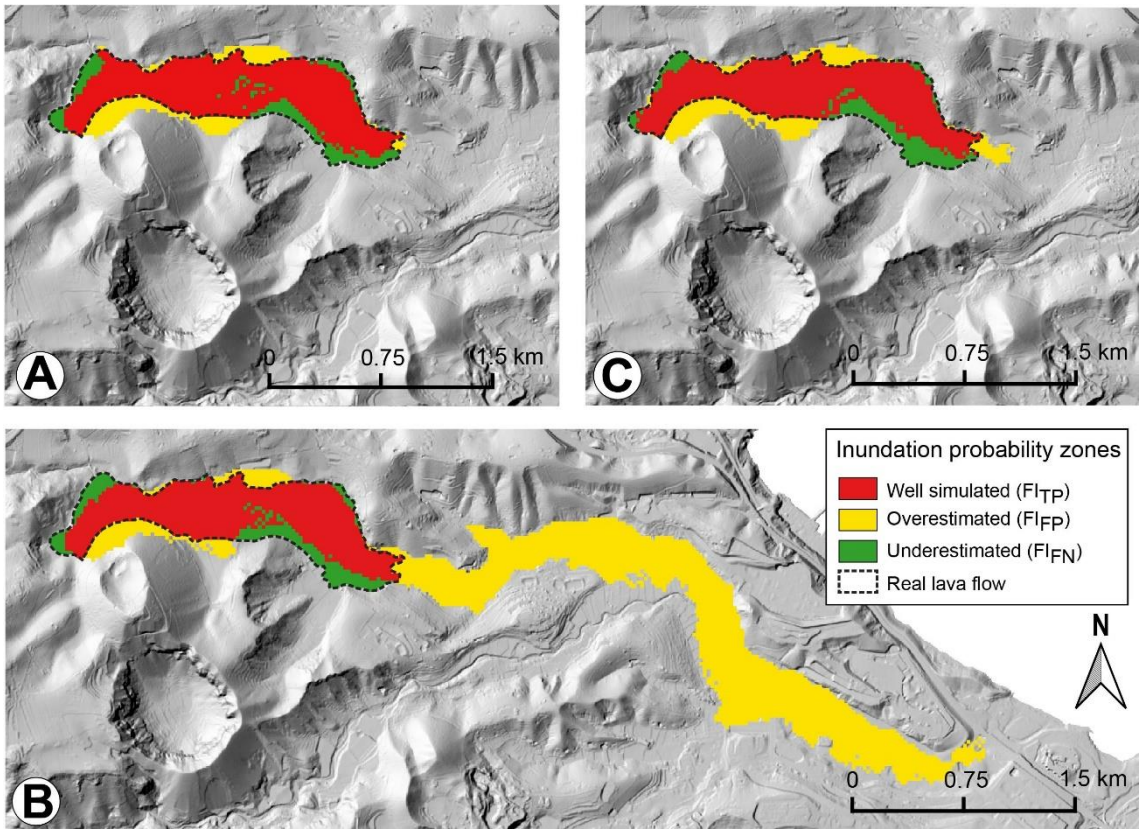

Figure 8.5. FI schematic representation where the overlap between real lava flow and simulated one is observed for L_{max} (A), Decreasing Probability (B) and FLOWGO (C) simulation models.

In all cases observed at Figure 8.5 it can be seen that a real lava flow large section coincides with the simulated one (red color), three overestimated areas (yellow color) and three underestimated ones (green color), although only two are significant, to the east and southeast of the actual lava flow limit. In the case of the overestimation located closest to emission center, the models have flooded pixels of the cone north flank, specifically inside the crater. In fact, in that area there is a small torrent of petrified lava whose study isn't contemplated to this work. Figure 8.5B, which shows *Decreasing Probability* model results, allows to observe a large extension of overestimated flow lines, or what is the same, those that the algorithm has generated and don't coincide with actual lava flow limits. On the other hand, Figures 8.5A and B hardly show significant differences, but analytically (Table 8.1) L_{max} model has an overlap percentage of 3.24 units greater, which, although it is not a very marked difference, is of a positive point for this.

Table 8.1. FI values as a percentage indicating the overlapping pixels' fraction.

Model	Well simulated pixels (%)	Overestimate pixels (%)	Underestimate pixels (%)
L_{max}	68.85	16.49	14.65
Decreasing Probability	28.71	64.19	7.10
FLOWGO	65.61	20.49	13.89

The L_{max} model is characterized by being the easiest to apply of the three. With only just need one parameter to work (lava flow length) whose determination is possible taking the actual lava flow measure, as well as minimum and average thickness calculated along the one. *Decreasing Probability* model has the lowest overlap percentage and it requires the lava flows mean and standard deviation record of all the Holocene eruptions that occurred in Gran Canaria. This model also needs the simulated flow extension, which in turn allows generating an overestimated area de 64.19% flooded pixels. That means that most of the simulated lava is outside real margins. Finally, in the *FLOWGO* model, numerous thermal, rheological and dynamic parameters must be introduced that simulate actual lava flow in a more approximate way and this is demonstrated in Table 8.1. However, the lava flow physic-chemical characteristics aren't usually known until it is expelled in a rash, and the computational processes are much slow. Therefore, the most suitable model for its efficiency in calculations is the L_{max}.

With this model, if the actual lava flow length isn't corrected, we can see how the front isn't able to complete the real lava flow path (Fig. 8.6A), contrary to what happens if the correction factor is applied in Figure 8.6B, where the front reaches a polygon eastern limit and even exceeds it in a few pixels. The conservation in the adequacy parameter FI is especially remarkable in this analysis because in Figure 8.6A the underestimated fraction is 0.28, not being flooded large number of pixels ($FI_{True\ Positive}$ lower) that yes they are in Figure 8.6B, decreasing the underestimated zone to a FI value of 0.16 and increasing the overlap.

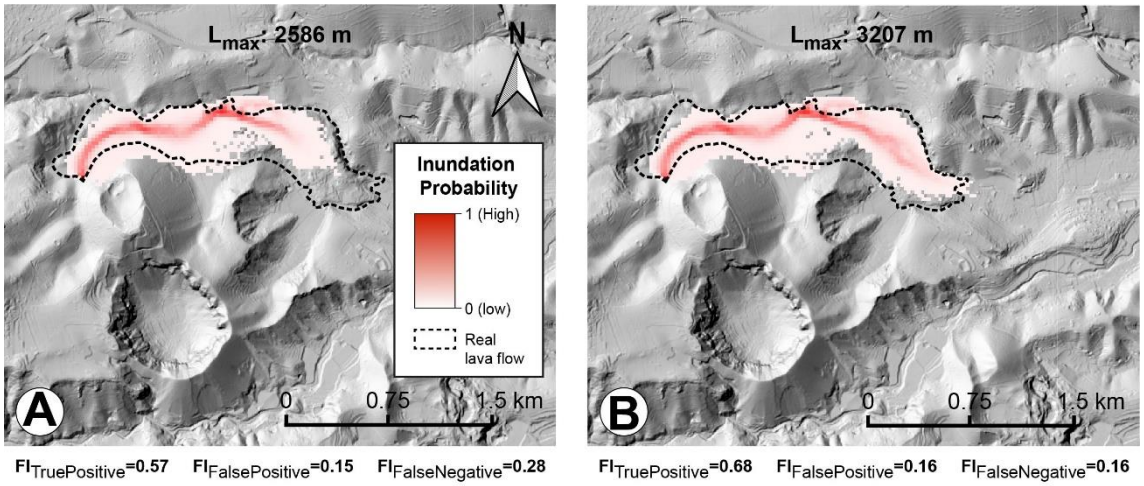

Figure 8.6. Lava flows simulation comparison from Pico de Bandama, assigning different values to L_{max},: without the correction factor value (A) and applied with 1.24 *(B).*

According to Mossoux *et al.* (2016), this fact is due to each flow line follows an irregular path whose length is longer than the shortest distance along the main lava flow channel. Similar observations are made when simulating lava flows on smoother slopes. So there may be a dependence between the intensity of the slope and the correction factor of the flow length.

8.3. DEM characteristics and its effects on simulations

When it comes to analyzing lava flow propagation on the same topography characterized by different DEMs, algorithm behavior to flooding each pixel can vary. The DEMs are the basis for the simulated flows and their resolution and morphology significantly influence the results.

The first implication of the DEM resolution is its impact on the parameter's initial values establishment, especially lava flow thickness. Mossoux *et al.* (2016), has shown that H_p optimal value is dependent on the resolution, varying with it. However, said values of H_p usually tends to real lava. On the other hand, H_p is of great importance, especially with the high resolution DEMs.

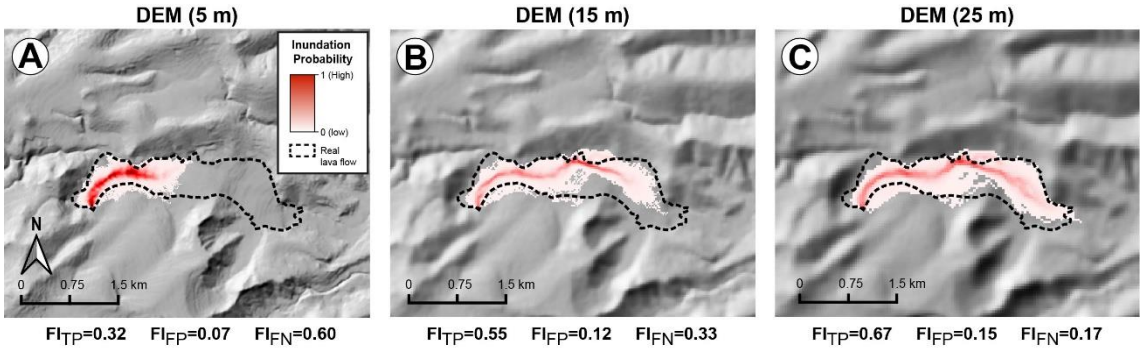

Figure 8.7. Lava flows flood probability results and FI values in DEMs with different resolution.

The following aspects to be discussed, in relation to the resolution, can be extracted from figure 8.7, which represents the Pico de Bandama lava flow simulating results using L_{max} model on different resolution DEMs. Figure 8.7A has the highest of all (pixels of 5x5 meters) that allow to see in detail lava flow geometry. This floods with a maximum probability ravine channel center, with a very adequate overlap during the first meters, until it stops abruptly. Simulated lava flow lines stop spreading even without having covered 60% of the pixels that make up real lava polygon (underestimated), being 32% full overlap. The flows over the DEMs of 15 and 25 m resolution (Fig. 8.7B and C, respectively) lose detail as it decreases, but gain in FI up to 67% (Fig. 8.7C). Thus, the lava flow length in the simulation decreases with increasing resolution. On the other hand, the processing time for each case is very variable, being larger the smaller the pixel size.

The second and last aspect to be studied is the DEM morphology since the lava flow flooding affects those areas with positive slopes (downwards) and flat areas. In the case of the Pico de Bandama eruption, land presented a different topography than the present one. The one corresponding to a paleosurface, where the "Barranquillo de Dios" didn't exist, but instead there was a ravine with characteristics more typical of a large valley with a "U" shape, through which the Pico de Bandama lava flowed, coinciding in 69% with the simulated lava, thanks to L_{max} model, as shown in figure 8.8A. The resulting relief results in a land relief inversion. The channel center becomes a watershed while the sides are new channels through which the water stream. In the case of figure 8.8B, lava simulation with the same characteristics on the current topography is represented, which would be a subsequent eruption to the one studied. The Pico de Bandama lava would be partially covered by the material of the new eruption, with the rest of the volume being diverted by the two channels described, mainly by the one located to the south, since flooding maximum probability is observed following this course. This implies that the overlap is less adequate and a FI of 0.47 (47%) is obtained.

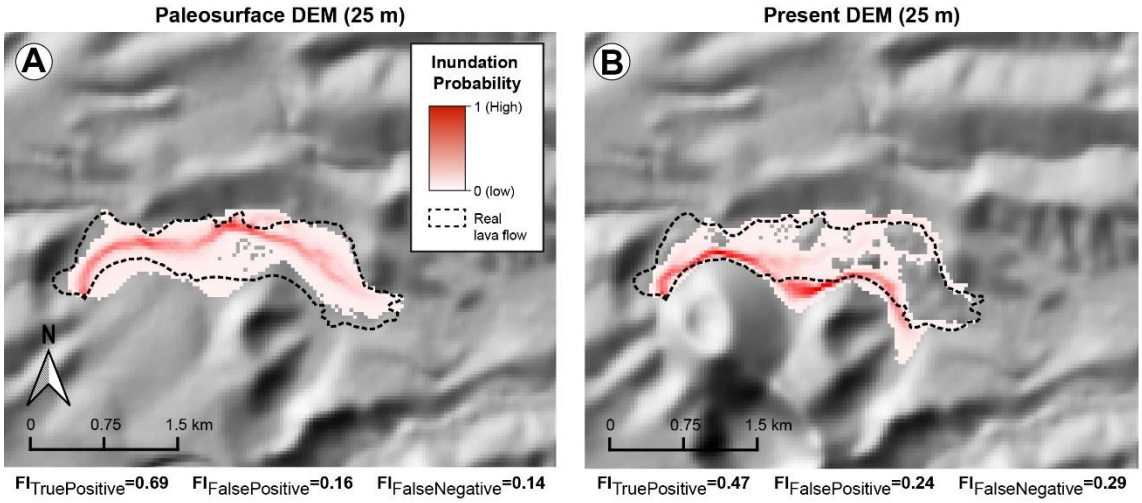

Figure 8.8. Lava flows flood probability results and FI values in DEMs with different topography.

9. CONCLUSIONS

Throughout this work it has been shown how GIS constitute a powerful tool in studies related to volcanology and volcanic hazard prevention. In Canary Islands, and specifically in Gran Canaria, the geological history, dominated by volcanism, is contemplated from its origins in Miocene (~14.5 Ma) to Holocene (at present). Therefore, a fundamental research methodology has been proposed to carry out subsequent volcanic hazard evaluation and management. On the one hand, digital maps have been manipulated to indicate Pico de Bandama volcanic units' cartography (volcanic cone, lava flow and pyroclastic mantle), whose eruption was chosen as an example due to its proximity in time (1970 ± 70 years ago) facing a future volcanic event. Geographical data and contour lines that form part of these units, have served to reconstruct surface affected by the volcanic activity in question (see section 4). With pre-eruption geomorphology it was determined that volcanic building was supported on gentle slope of a broad ravine with a "U" shape. Figure 9.1 B shows the present ravine appearance that was beyond lava front, conserving its smooth relief, about 2000 years ago. On the other hand, lava flow that flooded the channel allowed water to open up, striking the new surface. Specifically, it has run along lava flow sides, in its lateral contacts with ravine slopes. This rocky mass has ended up being a watershed. One of these flanks is composed by soft rock, thus water immediately dismantled this material, creating current Barranquillo de Dios, which is characterized by having very steep slopes that create "V" profile that has been observed in the field (Fig. 9.1 A).

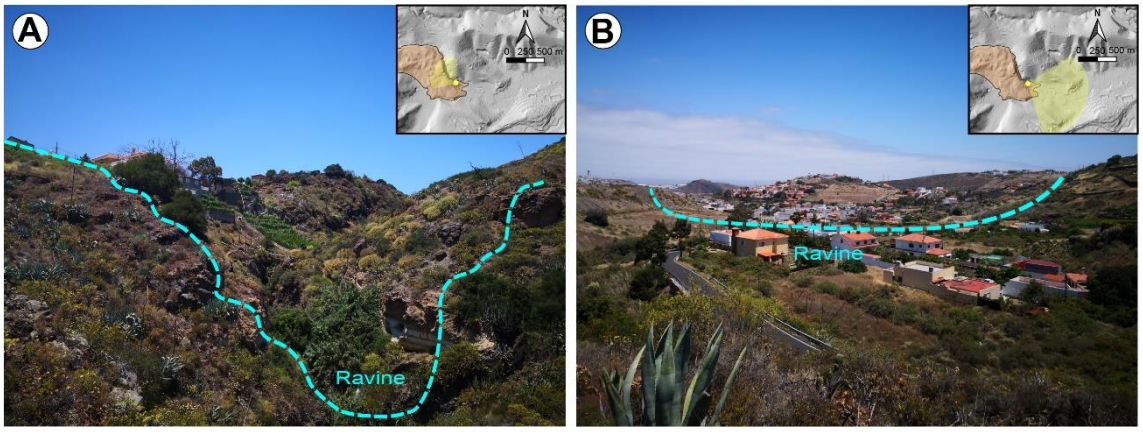

Figure 9.1. Lava flow view from its front towards interior, where it is incised by Barranquillo de Dios (A) and towards the outside, where it leaves ravine channel intact and with a soft morphology with less slope hillsides than in first case (B). In the upper right corner there is a DEM with laundry highlighted, indicating observation point and direction.

Pico de Bandama lava flooded ravine in reconstructed paleo-surface, flowing like a Bingham fluid. Its local movement and behavior was determined by simulations performed Q-LavHA application environment (see section 7). Different results were obtained comparing three different models: L_{max}, *Decreasing Probability* and *FLOWGO*. The calculation for each model could be developed with lava flow morphometric parameters and those relative to cone, to a lesser extent, (see section 8). Values influence of minimum and average thickness in the *FI* index was analyzed, as well as effects of laundry length, and DEM characteristics. *Decreasing Probability* model results were very inadequate for this study since in all the analyzes FI gave very low values. By contrast, L_{max}, and *FLOWGO* models proved to be adequate, first more than second by a small difference.

Results obtained with the adequate and optimized model and known Pico de Bandama lava characteristics ($H_c = 2\,m$; $H_p = 14\,m$) allowed to determine that flow would have flooded reconstrued channel in a similar way as it did time back, so if there were an eruption of similar characteristics, management plan would contemplate realistic hazard areas. With this information it could avoid personal injuries in the first place. On the other hand, it would avoid unnecessary media performance in areas that are low risk, since lava flow wouldn't reach it according to models studied.

APPENDIX

Appendix I - Standard and specific parameters used in *FLOWGO* model for Pico de Bandama eruption and its analytic results from optimal simulation.

FLOWGO model		
Standard parameters		**Pico de Bandama**
Vent coordinate (UTM zone 28N)	X	454614
	Y	3101837
DEM resolution (m)		25
H_c (m)		3
H_p (m)		14

Specific parameters	**Pico de Bandama**	***Fuente***
Lava flow speed		
Effusion rate (m^3/s)	100	*Estimated from several authors*
viscosity (Pa*s)	3.05	*Calculated* $\mu(\theta) = \mu i(1 - R\theta)^{-2,5}$
Initial phenocryst mass fraction	0.12	*Petrographically estimated*
Channel ratio (width/depth)	23.6	*Calculated from Rodriguez-González (2009)*
Thermal parameters		
T (eruption) (ºC)	1250	*Typical of very basic lavas*
T (crust) (ºC)	600	*Harris and Rowland (2001), Harris et al. (2015)*
Offset (ºC)	150	*Harris and Rowland (2001), Harris et al. (2015)*
d (constant)	-0.16	*Mossoux et al. (2016)*
Viscosity and elasticity		
a (constant) (1/K)	0.04	*Dragoni (1989)*
b (constant) (Pa)	0.01	*Dragoni (1989)*
c (constant) (1/K)	0.08	*Dragoni (1989*
Velocity constant		
Gravity (m/s^2)	9.81	-
Convenction parameters		
Wind speed (m/s)	5	*Harris and Rowland (2001)*

Ch (wind friction)	0.0036	*Harris and Rowland (2001)*
Convenction parameters		
Air temperature (ºC)	25	*Estimated*
Air density (kg/m^3)	0.4412	*Harris and Rowland (2001)*
Air specific heat capacity (J/kg.K)	1099	*Harris and Rowland (2001)*
Lava density and vesicularity		
DRE density (kg/m^3)	2906	*Calculated* $\rho = (1 - \theta b)\rho_{DRE}$
Vesicularity (%)	0.04	*Petrographically estimated*
Crystal parameters		
Growth rate	0.004	*Estimated from several authors*
L (J/kg)	350000	*Harris and Rowland (2001)*
R (inverse of the crystals maximum concentration)	1.51	-
Conduction parameters		
Thickness of lava crust (%)	10	*several authors*
T (base of lava crust) (ºC)	600	*several authors*
Lava termal conductivity (W/m.K)	2.05	*Cordonnier et al. (2014) and Mossoux et al. (2016)*
Radiation parameters		
Sbc (Stephan-Boltzmann constant) (W/m2.K4)	5.67E-08	-
e	0.95	*Harris and Rowland (2001); Cordonnier et al. (2014)*

Results (Fitness Index)

$FI_{true\ positive}$	0.66
$FI_{false\ positive}$	0.20
$FI_{false\ negative}$	0.14

Appendix II - Standard parameters used in L_{max} model for the Pico de Bandama eruption and its analytic results from optimal simulation.

L_{max} model		
Parameters		**Pico de Bandama**
Vent coordinate (UTM zone 28N)	X	454614
	Y	3101837
DEM resolution (m)		25
Lava flow length (m)		2585* · 1.24 = 3207
H_c (m)		2
H_p (m)		14
Results (Fitness Index)		
$FI_{true\ positive}$		0.68
$FI_{false\ positive}$		0.16
$FI_{false\ negative}$		0.14

(*) Lava flow maximum length measured

Appendix III - Standard parameters used in *Decreasing Probability* model for the Pico de Bandama eruption and its analytic results from optimal simulation.

Decreasing Probability model		
Parameters		**Pico de Bandama**
Vent coordinate (UTM zone 28N)	X	454614
	Y	3101837
DEM resolution (m)		25
H_c (m)		2
H_p (m)		14
Holocene lava flows length (m)		From 20 eruptions
mean		3793
Standard deviation		2702
Results (Fitness Index)		
$FI_{true\ positive}$		0.29
$FI_{false\ positive}$		0.64
$FI_{false\ negative}$		0.07

REFERENCES

Antenucci, J.C., Brown, K., Croswell, P.L., Kevany, M.J., Archer, H., 1991. Geographic Information Systems: a guide to the technology.

Burroughs, P.A., McDonald, A., 1986. Principles of geographical information systems for land resources assessment. Monographs on soil and resources survey.

Carracedo, J.C., 2008. El Volcán Teide (Tomo2), in: Claves Para La Interpretación de Las Formas Volcánicas. Ediciones y Promociones Saquiro, S.L., Santa Cruz de Tenerife, Canarias(España), pp. 7–64.

Carracedo, J.C., 2011. Geología de Canarias: Origen, evolución, edad y volcanismo. I. Editorial Rueda.

Clarke, K.C., 1986. Advances in geographic information systems. Computers, environment and urban systems 10, 175–184.

Cowen, D.J., 2003. GIS versus CAD versus DBMS: what are the differences?, in: Introductory Readings in Geographic Information Systems. CRC Press, pp. 70–80.

de Francisco, M., José, M., 2014. Algoritmo probabilístico para la simulación de flujos de lavas.

Department of the Environment, 1987. Handling geographic information.

Felicísimo, Á.M., 1994. Modelos digitales del terreno. Pentalfa Oviedo.

Guillou, H., Torrado, F.J.P., Hansen Machin, A.R., Carracedo, J.C., Gimeno, D., 2004. The Plio–Quaternary volcanic evolution of Gran Canaria based on new K–Ar ages and magnetostratigraphy. Journal of Volcanology and Geothermal Research 135, 221–246.

Hansen Machín, A., Rodriguez-Gonzalez, A., Perez-Torrado, F.-J., 2008. Vulcanismo Holoceno: Bandama y su entorno. Geo-Guías, 5. Itinerarios Geológicos por las Islas Canarias : Gran Canaria. Editores Francisco José Pérez Torrado y María del Carmen Cabrera, Sociedad Geológica de España, 978-84-930160-5-0, excursión intra-congreso, 4, p. 89-103.

Harris, A.J.L., Rowland, S.K., 2001. FLOWGO: a kinematic thermo-rheological model for lava flowing in a channel. Bulletin of Volcanology 63, 20–44.

Montelli, R., Nolet, G., Dahlen, F.A., Masters, G., Engdahl, E.R., Hung, S.-H., 2004. Finite-frequency tomography reveals a variety of plumes in the mantle. Science 303, 338–343.

Mossoux, S., Saey, M., Bartolini, S., Poppe, S., Canters, F., Kervyn, M., 2016. Q-LAVHA: A flexible GIS plugin to simulate lava flows. Computers & Geosciences 97, 98–109.

Mossoux, S., Saey, M., Bartolini, S., Poppe, S., Canters, F., Kervyn, M., 2017. Q-LAVHA 2.0: MANUAL.

Richardson, P., Karlstrom, L., 2019. The multi-scale influence of topography on lava flow morphology. Bulletin of Volcanology 81, 21.

Rielo, A.F., 2002. Modelización física y simulación numérica de procesos eruptivos para la generación de mapas de peligrosidad volcánica (PhD Thesis). Universidad Complutense de Madrid.

Rodríguez González, A., 2009. El vulcanismo holoceno de Gran Canaria: Aplicación de un sistema de información geográfico. Universidad de Las Palmas de Gran Canaria, Las Palmas de Gran Canaria.

Rodriguez-Gonzalez, A., Perez-Torrado, F.J., Fernandez-Turiel, J.L., Aulinas, M., Paris, R., Moreno-Medina, C., 2018. The Holocene volcanism of Gran Canaria (Canary Islands, Spain). Journal of Maps 14, 620–629.

Vera, J.A., 2004. Geología de España. Igme.

Vitturi, M. de'Michieli, Tarquini, S., 2018. MrLavaLoba: A new probabilistic model for the simulation of lava flows as a settling process. Journal of Volcanology and Geothermal Research 349, 323–334.

MEMORIA FINAL DEL TRABAJO FIN DE GRADO (TFG)

Grado en Ciencias del Mar. Asignatura:40630 – Trabajo Fin de Grado
Año académico: 2018/2019 Alumno: Airam Echedey Pérez Reyes

1. Descripción detallada de las actividades desarrolladas y formación recibida durante la realización del TFG

El periodo de elaboración del TFG abarcó desde el 29 de enero, junto con las prácticas curriculares, hasta el __ de Junio, comenzando con una recopilación bibliográfica para entrar en materia. Ello fue útil para la organización de la estructura del trabajo, que se fue perfeccionando con el paso de las semanas a medida que redactaba los contenidos. Posteriormente proseguí con unas lecciones básicas para aprender a utilizar el software de SIG, conocido como Q-GIS (Fig. 1.1). No era la primera vez que entraba en contacto con un software parecido, porque en la asignatura de "Técnicas de Información Geográfica en el Ámbito Geológico" del primer semestre, hice uso de uno parecido denominado TNTmips. La razón de no utilizar este último que ya manejaba con relativa soltura, consiste en que el plugin de simulación de flujos de lava Q-LavHA, usado en este TFG, ha sido creado para usar en el software de Q-GIS, que además es "software libre". Otras de las razones es que poco a poco, las administraciones públicas y empresas lo están introduciendo como software principal en SIG en detrimento de los softwares de pago. Con lo cual, el día de mañana, cuando sea insertado en el mundo laboral, me será más sencillo adecuarme a los métodos de trabajo de la empresa competente y estaré más cualificado para el puesto, al manejar el software que probablemente utilicen. Aunque quiero dejar claro en esta memoria que no es sólo saber manejar un software de SIG, sino entender la filosofía de SIG, independientemente el software que se use.

Figura 1.1. Logos del software de SIG, Q-GIS de dos versiones distintas: a la izquierda la versión más reciente cuando comencé las prácticas y a la derecha una versión previa necesaria para el uso en unas tareas.

Una vez sabía los procesos más sencillos y más comunes en Q-GIS, comencé con el aprendizaje de morfometría volcánica aplicando con herramientas de SIG para la

reconstrucción paleo-geomorfológica y topográfica de la erupción del Pico de Bandama. Concretamente hice un estudio en profundidad de la topografía en cuestión, tanto actual como la reconstruida. Para el último caso no sólo bastó con analizar superficies, sino que también hubo que reconstruirlas. En su caso, tomando un mapa topográfico digital con curvas de nivel y modificando una a una cada una de ellas. Todo ello teniendo en cuenta, las interpretaciones del terreno en las diferentes fases de reconstrucción (Fig. 1.2). Con todos los procedimientos completados, obtuve una tabla de parámetros morfométricos para el cono y la colada de lava de la erupción del Pico de Bandama, esenciales para llevar a cabo las simulaciones de flujo de lava.

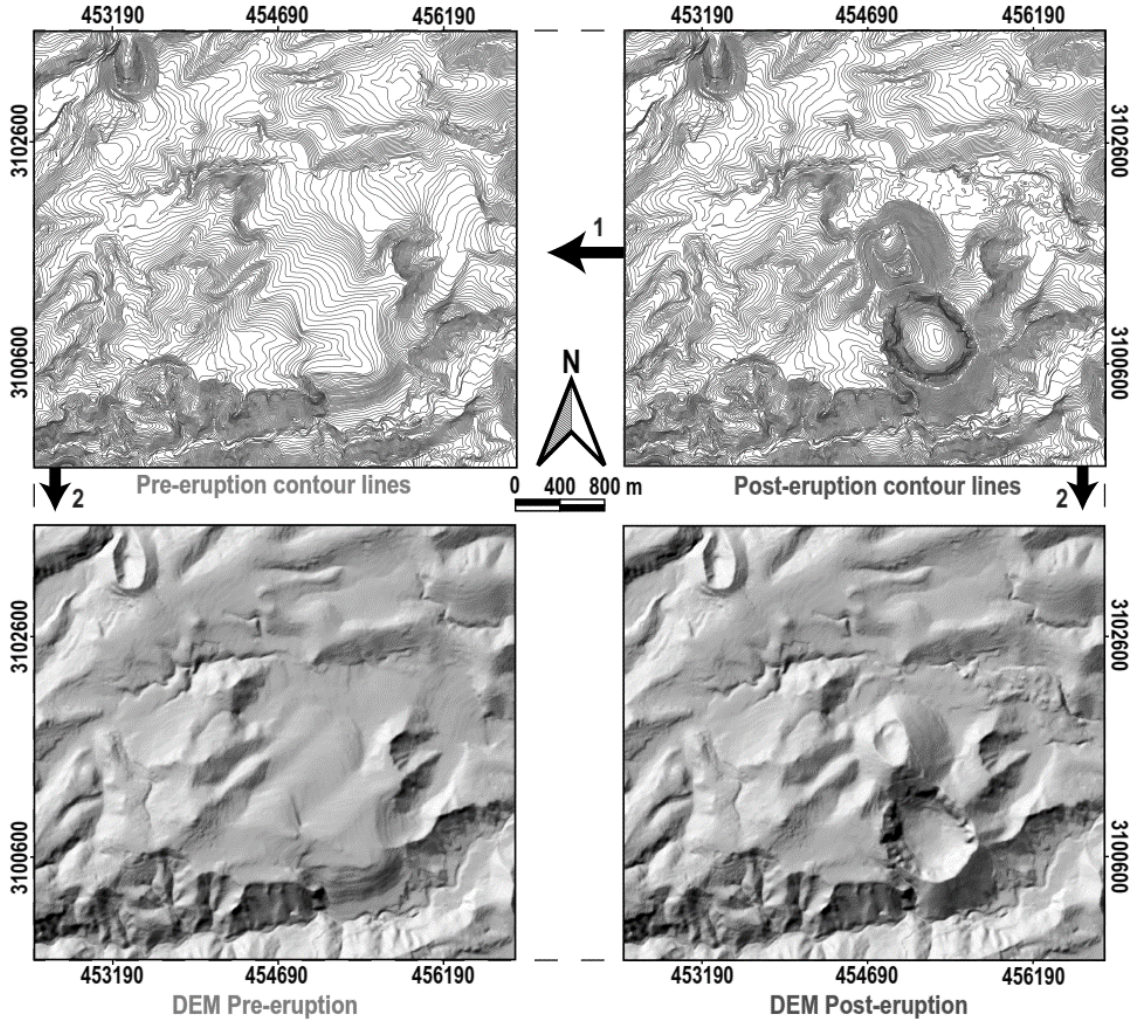

Figura 1.2. Comparación entre las superficies pre- y post-erupción del Pico de Bandama. A partir de un solo mapa de curvas de nivel actual (arriba izquierda) se procedió a reconstruir la topografía anterior a la erupción (Proceso 1). Con estos dos mapas se aplicó un algoritmo de interpolación (Proceso 2) con los que se obtuvieron los dos Modelos Digitales de Elevación (DEM) inferiores.

Para poder abordar la parte de simulación de flujos de lava también aprendí de forma intensiva a utilizar una aplicación (plugin) otro programa de SIG muy específico, llamado *Q-LavHA* que se ejecuta en el entorno de *Q-GIS* (Fig. 1.3). Este plugin simula la probabilidad de inundación de un flujo de lava canalizado sobre un Modelo Digital de Elevación (DEM sus siglas en inglés). Tiene la capacidad de generar simulaciones en base a tres modelos diferentes, dos probabilísticos y uno determinístico. Para el caso de los probabilísticos se aplicaron los datos obtenidos en el análisis morfométrico, pero para el segundo caso, hubo que recurrir a bibliografía, trabajo de campo y de taller, ya que los datos que se deben introducir también incluyen parámetros físico-químicos de la lava.

Figura 1.3. Logo del plugin Q-LavHA.

Por tanto, el Dr. Alejandro Rodríguez González me mostró el procedimiento para conseguir la información a partir de las muestras tomadas en el campo, el cual explicaré a continuación, en unos sencillos y breves pasos:

1. En el campo se toma mediante el martillo de geólogo un fragmento generoso de roca (Fig. 1.4), en este caso de la lava del Pico de Bandama, con un aspecto de roca fresca, es decir, con minerales lo menos alterados posible.

Figura 1.4. Muestra de roca de la colada de lava del volcán Pico de Bandama.

2. Ahora en el taller, se limpian las caras con una sierra especial y refrigerada con agua (Fig. 1.5A) y se corta en varios tacos de tamaño de unos 5x5 cm (Fig. 1.5B). De los cuales uno de ellos se envía a la Universidad de Barcelona para elaborar

una lámina delgada, que sirve para conocer datos como la vesicularidad y caracterización de minerales que componen la roca.

Figura 1.5. A) Imagen de la sierra operativa en el taller de Geología. B) Ejemplos de tacos de la muestra de roca de la lava del Pico de Bandama.

3. Se emplea la machacadora (Fig. 1.6A) con el resto de tacos obtenidos, introduciéndolos uno por uno en la máquina para obtener un tamaño grava (Fig. 1.6B).

Figura 1.6. A) Imagen de la machacadora del taller de Geología. B) Ejemplo del resultado de la muestra una vez machacados los tacos de roca.

4. Con un mortero de Ágata (Fig. 1.7) se va moliendo poco a poco los granos de roca obtenidos a partir de los tacos hasta conseguir un polvo homogéneo (con apariencia limo-arcillosa), parte del cual se envía a la Universidad de Barcelona para proceder a realizar los análisis geoquímicos oportunos.

Figura 1.7. Mortero de Ágata operativo en el taller de Geología.

No obstante, dado que las prácticas y el TFG se centran en la morfometría y las simulaciones de flujos de lava, este procedimiento y la toma de muestras en el campo de forma minuciosa, sólo se explicaron de forma teórica, con aplicación práctica directa en un proyecto de investigación de las mismas características que el llevado a cabo para este caso. Además, esta decisión implicó que utilizara los datos ya tomados en campañas de anteriores, y los proporcionados por las respectivas muestras enviadas a la Universidad de Barcelona, lo cual permitió ahorrar bastante tiempo y recursos económicos.

2. Nivel de integración e implicación dentro del departamento y relaciones con el personal

Durante mi periodo de desarrollo del TFG, se me brindó un puesto de trabajo en el Laboratorio de Geología (B-204), así como también la posibilidad de utilizar el Taller de Geología (sótano 1), ubicados ambos en el edificio de Ciencias Básicas (Campus Universitario de Tafira s/n, 35017-Las Palmas de Gran Canaria). Allí también se me facilitó el material de apoyo necesario para la correcta realización de las tareas previstas: un ordenador propio con dos monitores (Fig. 1.8), disponibilidad de bibliografía específica y material de trabajo de campo (GPS, martillo, bolsas de muestras de roca, etc.).

Figura 1.8. Imagen del puesto de trabajo asignado en el Laboratorio de Geología (B-204), con ordenador y dos monitores.

Al menos en las primeras semanas estuve totalmente solo. Sin embargo, posteriormente compartí el espacio de trabajo con la estudiante Laura Arencibia Pérez. Ella también cursaba las prácticas curriculares, pero en colaboración con el grupo GEOGAR, dentro del Instituto de Oceanografía y Cambio Global (IOCAG). Cabe destacar que es una persona con la que he entablado una buena relación, respetuosa y cortés. Además, ha resultado ser de gran ayuda, pues cualquier duda burocrática relacionada con el proceso de seguimiento de tanto del TFG, como de prácticas, la he consultado con ella. Por mi parte he podido también apoyarla con temas relacionados con el TFG como, por ejemplo, elaboración de mapas de diversa índole y edición de imágenes.

3. Aspectos positivos y negativos más significativos relacionados con el desarrollo del TFG

El hecho de mantener una mente abierta respecto a las otras ciencias mientras redactaba las líneas del trabajo, y realizaba los análisis de la topografía del Pico de Bandama y simulaciones de flujo de lava, lo considero un aspecto muy positivo. También lo es la principal razón que me fascine la Vulcanología y en general la Geología, las aplicaciones directas de conceptos teóricos, y además que se puedan visualizar de una manera única. En muchos trabajos realizados durante el grado, siempre se he recurrido a bibliografías, solo reinterpretando conceptos ya explicados anteriormente y plasmándolos en otro documento nuevo. Pero en las asignaturas de Geología, desde el primer año, la gran mayoría de las veces me he entretenido recreando procesos, imaginando unos nuevos, y estudiando el estado actual de la Geomorfología de la Tierra. Este trabajo específico no fue una excepción, porque en ningún momento me he aburrido al modelizar la erupción holocena que se escogió de ejemplo: el Pico de Bandama, última erupción

ocurrida en la isla de Gran Canaria y de la que los aborígenes fueron testigos (y posiblemente víctimas). A ello se unió el buen ambiente con los docentes, a los cuales se les nota verdadera pasión por lo que hacen. Por otro lado, lo que si destaco como un aspecto negativo es el equipo informático, y los problemas computacionales que he tenido durante este tiempo, entre el mío propio y el cedido por el grupo GEOVOL, pero no supusieron mayor contratiempo que dedicar unas horas de más para solucionarlos y de paso aprender un poco más sobre informática (hardware y software). Otro aspecto negativo a tener en cuenta es la información incompleta cedida a los estudiantes durante el transcurso del semestre, ya que no quedó claro la realización de una temporalización, los aspectos a tener en cuenta en ella, el formato variable del propio trabajo, pudiendo ser bibliográfico o tipo artículo científico. Sin embargo, me ha parecido significativa la colaboración del equipo docente para solucionar dudas respecto a ello y sin duda su apoyo es un aspecto positivo.

4. Valoración personal del aprendizaje conseguido a lo largo del TFG

Del aprendizaje que han supuesto estos meses, comienzo explicando que sólo tengo la intención de poder continuar estudiando Geología o mejor aún, ocupando una plaza laboral en algún otro momento de mi vida si surge la oportunidad. Volviendo a lo aprendido durante el desarrollo del trabajo, no me costó demasiado arrancar motores, siempre he sido una persona muy proactiva en el comienzo de cualquier proyecto o etapa nueva que se me presenta. El verdadero reto que noté fue mantener el ritmo, siguiendo asimilando procesos computacionales y aplicarlos de forma correcta, uno detrás de otro. Había días en los que después de una tutoría en la que me explicaban muchos de ellos, la cabeza no me daba para más y no continuaba con las tareas hasta el día siguiente, cuando estaba más fresco y con la ayuda de un guión de pasos y tareas a seguir bien definido y estructurado. Ahí es donde avanzaba, con decisión a completar cada fase de las reconstrucciones.